

LA-UR-17-22084 (Accepted Manuscript)

Mixed valent metals

Riseborough, P. S. Lawrence, Jon M.

Provided by the author(s) and the Los Alamos National Laboratory (2017-12-14).

To be published in: Reports on Progress in Physics

DOI to publisher's version: 10.1088/0034-4885/79/8/084501

Permalink to record: http://permalink.lanl.gov/object/view?what=info:lanl-repo/lareport/LA-UR-17-22084

Approved for public release. Los Alamos National Laboratory, an affirmative action/equal opportunity employer, is operated by the Los Alamos National Security, LLC for the National Nuclear Security Administration of the U.S. Department of Energy under contract DE-AC52-06NA25396. Los Alamos National Laboratory strongly supports academic freedom and a researcher's right to publish; as an institution, however, the Laboratory does not endorse the viewpoint of a publication or guarantee its technical correctness.



REPORT ON PROGRESS

Mixed valent metals

To cite this article: P S Riseborough and J M Lawrence 2016 Rep. Prog. Phys. 79 084501

Manuscript version: Accepted Manuscript

Accepted Manuscript is "the version of the article accepted for publication including all changes made as a result of the peer review process, and which may also include the addition to the article by IOP Publishing of a header, an article ID, a cover sheet and/or an 'Accepted Manuscript' watermark, but excluding any other editing, typesetting or other changes made by IOP Publishing and/or its licensors"

This Accepted Manuscript is © © 2016 IOP Publishing Ltd.

During the embargo period (the 12 month period from the publication of the Version of Record of this article), the Accepted Manuscript is fully protected by copyright and cannot be reused or reposted elsewhere.

As the Version of Record of this article is going to be / has been published on a subscription basis, this Accepted Manuscript is available for reuse under a CC BY-NC-ND 3.0 licence after the 12 month embargo period.

After the embargo period, everyone is permitted to use copy and redistribute this article for non-commercial purposes only, provided that they adhere to all the terms of the licence https://creativecommons.org/licences/by-nc-nd/3.0

Although reasonable endeavours have been taken to obtain all necessary permissions from third parties to include their copyrighted content within this article, their full citation and copyright line may not be present in this Accepted Manuscript version. Before using any content from this article, please refer to the Version of Record on IOPscience once published for full citation and copyright details, as permissions will likely be required. All third party content is fully copyright protected, unless specifically stated otherwise in the figure caption in the Version of Record.

View the article online for updates and enhancements.

Mixed Valent Metals

P.S. Riseborough Temple University, Philadelphia, Pa 19122 J.M. Lawrence Los Alamos National Laboratory, Los Alamos, NM 87545 March 9, 2016

Abstract

We review the theory of mixed-valent metals and make comparison with experiments. A single-impurity description of the mixed-valent state is discussed alongside the description of the nearly-integer valent or Kondo limit. The degeneracy N of the f-shell plays an important role in the description of the low-temperature Fermi-liquid state. In particular, for large N, there is a rapid cross-over between the mixed-valent and the Kondo limit when the number of f electrons is changed. We discuss the limitations on the application of the single-impurity description to concentrated compounds such as those caused by the saturation of the Kondo effect and those due to the presence of magnetic interactions between the impurities. This discussion is followed by a description of a periodic lattice of mixed-valent ions, including the role of the degeneracy N. The article concludes with a comparison of theory and experiment. Topics covered include the single-impurity Anderson Model, Luttinger's theorem, the Friedel sum rule, the Schrieffer-Wolff transformation, the single-impurity Kondo Model, Kondo Screening, the Wilson Ratio, Local Fermi-Liquids, Fermi-liquid sum rules, the Noziéres exhaustion principle, Doniach's Diagram, the Anderson Lattice Model, the Slave-Boson Method, etc.

1 Introduction

Mixed valence or intermediate valence is a concept introduced to describe the characteristic features of the electronic states of atoms in a solid with partially filled, almost localized configurations that are nearly degenerate. Mixed-valent compounds include those which are inhomogeneous, i.e. where atoms with differing static valence reside on inequivalent sites of the crystal, and those for which the valence is homogeneous, with the same non-integral value on each site. The latter, which are often referred to as intermediate-valence compounds, are the topic of this paper. This review, which is intended to be pedagogical, addresses a subject that has developed over fifty years, and focuses on the basic concepts of mixed

valence.

Mixed-valence frequently occurs in compounds containing elements at the beginning, middle and end of the lanthanide series. In the lanthanide materials, the 4f-orbitals are partially filled, spatially located inside the outer atomic (5d6s) shell and, therefore, are less sensitive to the effects of external perturbations and experience fairly strong intra-atomic Coulomb interactions. The properties of most compounds containing lanthanide elements can be described in terms of almost localized $(4f)^n$ orbitals with a valence band which is derived from the $(5d6s)^m$ shell. A discussion of the normal rare-earth compounds can be found in the book by Coqblin [1]. The anomalous rare earths are those in which two or more configurations are nearly degenerate, so the effect of perturbations due to the crystalline environment produces a state which is a linear superposition of the configurations [2]. For example, the electronic state on an atom $|\psi\rangle$ can be crudely thought of as being composed of the linear superposition of electrically neutral atomic states

$$|\psi\rangle = a | (4f)^n (5d6s)^m\rangle + b | (4f)^{(n+1)} (5d6s)^{m-1}\rangle$$
 (1)

where a and b are complex numbers, n and m are integers. The state is normalized to unity if

$$|a|^2 + |b|^2 = 1.$$
 (2)

The number representing the average valence \boldsymbol{v} of this state is expressed as

$$v = |a|^{2} m + |b|^{2} (m - 1)$$

$$= m - |b|^{2}$$

$$= (m - 1) + |a|^{2}.$$
(3)

When a and b are both non-zero, the system has a mixed or non-integer valence, whereas if only one number from the pair a and b is non-zero, the system is integer valent. The stability of open and closed shells leads to mixed-valence being found in materials containing Ce and Yb. For Ce mixed-valent compounds, the relevant configurations are

$$|\psi_{Ce}\rangle = a |(4f)^{0} (5d6s)^{4}\rangle + b |(4f)^{1} (5d6s)^{3}\rangle$$
 (4)

for which the valence is intermediate between 4 and 3. Likewise, for Yb mixed-valence compounds, one has

$$|\psi_{Yb}\rangle = a |(4f)^{14} (5d6s)^2\rangle + b |(4f)^{13} (5d6s)^3\rangle$$
 (5)

so the valence may be intermediate between 2 and 3. The Ce and Yb compounds are frequently thought of as being f electron - hole symmetric partners, connected by the transformation $n_f \to (14 - n_f)$. The half-filled 4f shell $(4f)^7$ is stabilized by the Hund's rule exchange and can lead to the formation of Sm and Eu mixed-valent materials. The rare-earth heavy-fermion materials are all, to some extent, mixed-valent. Although the heavy-fermion systems with the highest effective masses are close to

the integer valent limit, the not-so-heavy systems (such as $CePd_3$) are more mixed-valent. Since the description of mixed-valence involves partially filled $(4f)^n$ shells which are almost localized, they should be subject to Hund's rule correlations and, therefore, may posses a degeneracy associated with the magnetic 4f configurations.

2 A Localized Paradigm

The anomalous nature of the mixed-valent lanthanide compounds is clearly seen through inspection of their magnetic properties. The integer-valent lanthanide metals usually posses 4f magnetic moments that are primarily governed by the atomic Hund's rule correlations and crystalline electric field splittings. Generally, the strength of the local interactions are considered to follow the hierarchy composed of the direct Coulomb interactions U and the Coulomb exchange interactions J between pairs of 4f electrons on the same ion, the spin-orbit interaction, followed by the splittings produced by the crystalline electric field. The local 4f magnetic moments are coupled by the Ruderman-Kittel-Kasuya-Yosida (RKKY) interaction involving the electrons in the conduction band [3, 4, 5]. In the RKKY mechanism, a 4f magnetic moment produces a polarization in the conduction band electrons which then propagates to a neighboring 4f magnetic moment and interacts with it. Since this indirect interaction between the 4f moments primarily involves producing a polarization of the conduction electron states near the Fermi-level, the RKKY interaction is oscillatory with a period governed by the $2k_F$ momentum transfer cutoff imposed by the Fermi-surface. The RKKY interaction causes the localized moments of the integer-valent rare earths to order magnetically, thereby lifting much of the degeneracy associated with the array of local 4f moments. By contrast, the mixed-valent compounds are frequently found to be paramagnetic. Since, for both Ce and Yb compounds, one 4f configuration has a magnetic moment and the other is non-magnetic, it is natural to ask "What are the magnetic properties associated with a localized (magnetically degenerate) state that couples to a non-magnetic (non-degenerate) state?" A model that describes this situation was formulated by P.W. Anderson [6].

3 Single-Impurity Models

A simple model that describes a mixed-valent state is given by the single-impurity Anderson Model [6]. The model consists of an f level localized on the impurity site, which hybridizes with a conduction band. The Hamiltonian can be written as the sum

$$\hat{H} = \hat{H}_f + \hat{H}_d + \hat{H}_{fd} \tag{6}$$

where \hat{H}_f governs the f electrons, \hat{H}_d describes the conduction band and \hat{H}_{fd} describes the hybridization process. The localized f orbital is de-

scribed by a Hamiltonian \hat{H}_f

$$\hat{H}_f = \sum_{\alpha} E_{f,\alpha} f_{\alpha}^{\dagger} f_{\alpha} + \frac{U}{2} \sum_{\alpha \neq \beta} f_{\alpha}^{\dagger} f_{\alpha} f_{\beta}^{\dagger} f_{\beta}$$
 (7)

where f_{α}^{\dagger} , f_{α} , respectively, create and destroy an electron on the impurity site on the f-orbital labeled by α , $E_{f,\alpha}$ is the binding-energy and U is the screened Coulomb interaction between pairs of f electrons on the impurity site. The factor of one-half in the Coulomb interaction term is introduced so that the interaction energy U between each pair of electrons is only counted once in the double summation. The index α represents the combined spin and orbit quantum numbers which run over N values. The effect of the spin-orbit coupling is assumed to lift the fourteen-fold degeneracy of the ionic 4f states, reducing it to an effective degeneracy N given by either six for Ce or eight for Yb. Generally, for most mixed-valent metals, the crystalline electric field is neglected since the splittings it produces are smaller than the widths introduced by the mixing of 4f configurations. However, for systems with large crystalline field splittings the value of Ncan be replaced by the degeneracy of the lowest crystal field level. We assume that the system is invariant under special unitary transformations SU(N) of the basis states labeled by α . The Pauli-principle excludes an interaction between a pair of electrons in the same single-particle state $\alpha = \beta$. A generalization of the form of the spin-rotationally invariant Coulomb interaction to the case of degenerate orbitals can be found in reference [7]. The direct and exchange Coulomb interactions ought to depend on the spin and orbital indices. The conduction electrons are described by H_d given by

$$\hat{H}_d = \sum_{\underline{k},\alpha} \epsilon_d(\underline{k}) \ d_{\underline{k},\alpha}^{\dagger} \ d_{\underline{k},\alpha} \tag{8}$$

where $d_{\underline{k},\alpha}^{\dagger}$, $d_{\underline{k},\alpha}$, respectively, create and destroy an electron in the Bloch state labeled by wavevector \underline{k} and quantum number α with the single-particle Bloch energy $\epsilon_d(\underline{k})$. The f states are coupled to the conduction states by the hybridization term \hat{H}_{fd} , given by

$$\hat{H}_{fd} = \frac{1}{\sqrt{N_s}} \sum_{k,\alpha} \left(V(\underline{k}) f_{\alpha}^{\dagger} d_{\underline{k},\alpha} + V^*(\underline{k}) d_{\underline{k},\alpha}^{\dagger} f_{\alpha} \right)$$
(9)

where N_s is the number of sites in the host crystal. The index α is assumed to be conserved since the model is invariant under SU(N). The first term describes a process whereby a conduction electron makes a transition from the Bloch state labeled by the Bloch wave vector \underline{k} and index α to the state of the localized f orbital labeled by the index α . The second term represents the time-reversed process. The quantity $V(\underline{k})$ is known as the hybridization matrix element.

3.1 The non-interacting (U=0) limit.

In the absence of the Coulomb interaction U, the model describes the Friedel virtual-bound state and the model is exactly soluble. The f density

of states is given by

$$\rho_f(\omega) = -\frac{1}{\pi} \sum_{\alpha} \Im \left(\frac{1}{\omega + i\eta - E_{f,\alpha} - \frac{1}{N_s} \sum_{\underline{k}} \frac{|V(\underline{k})|^2}{\omega + i\eta - \epsilon_d(\underline{k})}} \right)$$
(10)

in the limit $\eta \to 0$. The real part of the quantity

$$S(\omega) = \frac{1}{N_s} \sum_{\underline{k}} \frac{|V(\underline{k})|^2}{\omega + i\eta - \epsilon_d(\underline{k})}$$
 (11)

can be thought of as a frequency dependent shift of the f level binding energy which is produced by the hybridization, and the imaginary part reduces to

$$\Im m \ S(\omega) = -\frac{\pi}{N_s} \sum_{\underline{k}} |V(\underline{k})|^2 \ \delta(\omega - \epsilon_d(\underline{k}))$$
 (12)

which is half the Fermi-Golden decay rate for an electron placed in the f-orbital due to the hybridization process whereby the electron leaks into the conduction band. Thus, if one ignores the frequency-dependence and sets

$$S(\omega) \approx \Delta E_f - i \pi \Delta \tag{13}$$

the f density of states has an approximate Lorentzian form. The conduction band density of states is also modified by the hybridization with the impurity level and is evaluated as

$$\rho_{d}(\omega) = \sum_{\underline{k},\alpha} \delta(\omega - \epsilon_{d}(\underline{k})) + \frac{1}{\pi} \sum_{\alpha} \Im \left(\frac{\partial}{\partial \omega} \frac{S(\omega)}{\omega + i\eta - E_{f,\alpha} - S(\omega)} \right)$$
(14)

where the second term vanishes if the f density of states is approximated by a Lorentzian. The total density of states is given by

$$\rho_{f}(\omega) + \rho_{d}(\omega) = \sum_{\underline{k},\alpha} \delta(\omega - \epsilon_{d}(\underline{k})) - \frac{1}{\pi} \sum_{\alpha} \Im \frac{\partial}{\partial \omega} \ln \left(\omega + i\eta - E_{f,\alpha} - S(\omega)\right).$$
(15)

Since the term involving the derivative has a single pole with unit residue, the total number of states is unaffected by the hybridization in accordance with Levinson's theorem [9].

The Friedel sum rule [10] relates the phase shift of the conduction electrons $\delta_{\alpha}(\epsilon)$ with quantum number α to the change in the density of states $\Delta \rho(\epsilon)$ via

$$\Delta \rho(\epsilon) = \frac{1}{\pi} \sum_{\alpha} \frac{\partial \delta_{\alpha}(\epsilon)}{\partial \epsilon} . \tag{16}$$

Therefore, the change in the number of electrons caused by the introduction of the impurity is given by

$$n_{imp} = \sum_{\alpha} \left(\frac{\delta_{\alpha}(\mu) - \delta_{\alpha}(-\infty)}{\pi} \right). \tag{17}$$

If the impurity carries an excess charge of ΔZ relative to the host metal, then local electrical neutrality requires that

$$\Delta Z = n_{imp} . (18)$$

For the approximation in which $S(\omega)$ is assumed to be independent of ω , $\Delta \rho(\omega)$ is entirely of f character and one has the relation

$$\Delta Z = n_T \tag{19}$$

with the total number of f electrons n_T .

The single-impurity Anderson model has been studied extensively, including exact solution by numerical renormalization group [11] and by Bethe Ansatz [12, 13, 14]. A comprehensive review can be found in a book by Hewson [15]. Here, we shall restrict our attention to only the most transparent descriptions of physical properties.

3.2 A Mean-Field Description

Anderson examined the condition under which local moments should form by using a mean-field description, in which the interaction term was linearized in the deviation $\Delta n_{f,\alpha}$ of the f electron number operator $\hat{n}_{f,\alpha} = f_{\alpha}^{\dagger} f_{\alpha}$ from its ground expectation value $\overline{n}_{f,\alpha} = \langle | f_{\alpha}^{\dagger} f_{\alpha} | \rangle$. The deviation operators are defined by

$$\Delta n_{f,\alpha} = \hat{n}_{f,\alpha} - \overline{n}_{f,\alpha} . \tag{20}$$

The mean-field Hamiltonian is found by replacing the Coulomb interaction

$$\hat{H}_{int} = \frac{U}{2} \sum_{\alpha \neq \beta} n_{f,\alpha} n_{f,\beta}
= \frac{U}{2} \sum_{\alpha \neq \beta} \left(\Delta n_{f,\alpha} \Delta n_{f,\beta} + \Delta n_{f,\alpha} \overline{n}_{f,\beta} + \overline{n}_{f,\alpha} \Delta n_{f,\beta} + \overline{n}_{f,\alpha} \overline{n}_{f,\beta} \right)$$
(21)

with

$$\hat{H}_{int}^{MF} = \frac{U}{2} \sum_{\alpha \neq \beta} \left(\Delta n_{f,\alpha} \, \overline{n}_{f,\beta} + \overline{n}_{f,\alpha} \, \Delta n_{f,\beta} + \overline{n}_{f,\alpha} \, \overline{n}_{f,\beta} \right)
= \frac{U}{2} \sum_{\alpha \neq \beta} \left(\hat{n}_{f,\alpha} \, \overline{n}_{f,\beta} + \overline{n}_{f,\alpha} \, \hat{n}_{f,\beta} - \overline{n}_{f,\alpha} \, \overline{n}_{f,\beta} \right)$$
(22)

in which one has neglected terms of second-order in the deviation operators. The last term is simply a real number which prevents over-counting

the contribution of the interaction to the total energy. The mean-field approximation simply results in the modification of the non-interacting model by the replacement

$$E_{f,\alpha} \rightarrow E_{f,\alpha} + U \sum_{\beta \neq \alpha} \overline{n}_{f,\beta}$$
 (23)

which simply shifts the position of the α -th f orbital due to its interaction with the average number of electrons in the other f orbitals.

In the Lorentzian approximation, the number $\overline{n}_{f,\alpha}$ is evaluated as

$$\overline{n}_{f,\alpha} = \frac{1}{\pi} \cot^{-1} \left(\frac{E_{f,\alpha} + U \sum_{\beta \neq \alpha} \overline{n}_{f,\beta} - \mu}{\Delta} \right)$$
 (24)

which is consistent with the Friedel sum rule. Therefore, it is found that, in general, the self-consistency equations form a set of N coupled transcendental equations.

For the case where the f level is degenerate, one has a solution corresponding to the state being fully degenerate, in which $\overline{n}_{\alpha} = \frac{n_T}{N}$ for all α where n_T is the total number of electrons in the f level. If one introduces the parameter $\theta = \frac{2 \pi n_T}{N}$, the self-consistency equation can be written as

$$\cot \frac{\theta}{2} = \left(\frac{E_f - \mu}{\Delta}\right) + \left(\frac{U(N-1)}{2\pi\Delta}\right)\theta \tag{25}$$

which always has a solution with positive θ . This solution corresponds to a state with unbroken symmetry. There are other solutions in which the symmetry is broken. The boundaries of the regions of $(\frac{E_f - \mu}{U})$ and $\frac{\Delta}{U}$ phase space where the symmetric solutions first become unstable are determined parametrically by the equations

$$\frac{1}{2\pi} \left(1 - \cos \theta \right) = \frac{\Delta}{U}$$

$$\frac{1}{2\pi} \left((N-1) \theta - \sin \theta \right) = \left(\frac{\mu - E_f}{U} \right). \tag{26}$$

The first equation shows that the tendency for symmetry breaking is greatest when the f orbitals are nearly half-filled and it sets the minimum value of $\frac{U}{\Delta}=\pi$ required to produce symmetry breaking. It should be noted that as N increases, the minimum value of U required to produce a broken symmetry increases rapidly for a nearly empty or nearly filled f shell, since

$$\frac{U_c}{\Delta} = \frac{\pi}{\sin^2(\frac{\pi n_T}{N})} \ . \tag{27}$$

Hence, the critical value U_c for local moment formation with $n_T \approx 1$ scales as N^2 . Although other terms of the Coulomb interactions between the f electrons (such as Hund's rule exchange and the pair hopping terms) may alter this criterion [8], since we are primarily concerned with occupancies of either around unity for Ce or around (N-1) for Yb, their effects on

the broken symmetry state may be considered negligible. The case with N=2 was considered by Anderson and corresponds to the spin-only degenerate model, in which case the broken symmetry state is magnetic. The magnetic moments are non-integral but, like the magnetic moments on isolated ions, are localized and should be invariant under rotations. For larger values of N, linear stability analysis shows that there are (N-1) possible linearly independent symmetry breaking modes.

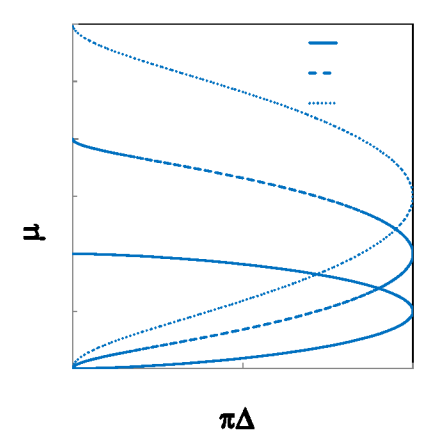
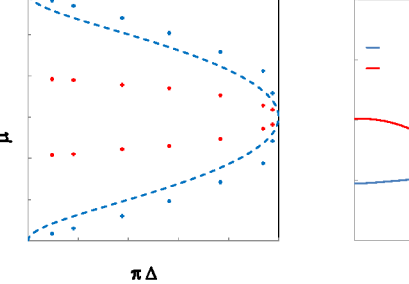


Figure 1: The $E_f - \mu$, Δ phase diagram, for various values of the degeneracy N. The broken symmetry phases are enclosed by the abscissa and the lines. Note that the phase diagram is symmetric under the f electron-hole exchange, $n_f \rightarrow N - n_f$.

The phase diagram for N=4, including some possible broken symmetry phases, is shown in the left panel of fig.(2). For large U, phase I corresponds to having a low energy singlet and a higher energy set of triplet states, whereas phase II corresponds to two sets of doublet states. Phase I* corresponds to the electron hole analogue of phase I. Typical one-electron density of states for phases I and II are shown in fig.(3). Symmetry breaking is accompanied by a quite sizeable change in the occupation of the flevel Δn_T from the value in the symmetric state. For example, the right panel of fig.(2) shows the Hartree-Fock energy $E(n_T, m)$ as a function of the symmetry breaking parameter m, where n_T is minimized at m=0 and n_T is minimized simultaneously with m, for which $\Delta n_T=0.2$.

The resulting violation of electrical neutrality in the vicinity of the impurity [10] indicates that the model should be generalized to include a screening of the local charge by the conduction electrons [16]. The effect of screening is not expected to play an important role in concentrated compounds, since the change in f occupation is expected to result in a change in the chemical potential which will produce a change in the number of conduction electrons.



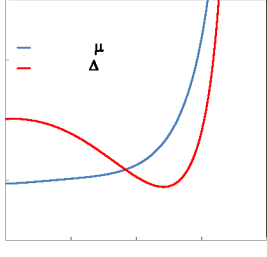


Figure 2: (Left Panel) The $E_f - \mu$, Δ phase diagram, for N=4. The broken symmetry phases for large U are composed of regions I, in which there is a low-energy singlet and a higher energy set of triplet states, region II where there are two sets of two doublet states, and I* which is the electron-hole analogue of region I. (Right Panel) The Hartree-Fock energy $E(n_T, m)$ as a function of m for the case in which n_T is minimized at m=0 and the case where n_T and m are simultaneously minimized. The values $\frac{E_f}{U}$ and $\frac{\Delta}{U}$ used put the system close to the boundary between the paramagnetic phase and phase I, as denoted by the blue symbols in the left panel.

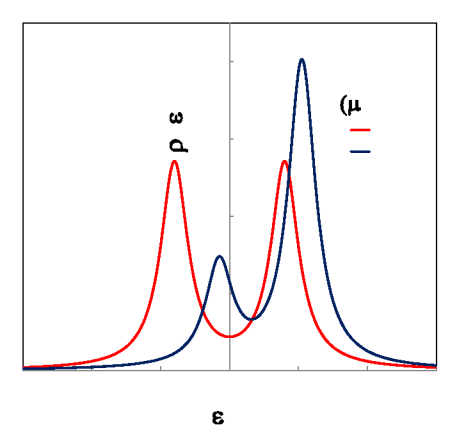


Figure 3: Typical one-electron spectral densities for the N=4 broken-symmetry phases, I and II in which the four f-levels either split into a singlet and triplet (I) or two doublets (II).

In the rare earth series, the spin-orbit splitting is large, with a magnitude of about 0.25 eV for Ce and 1.5 eV for Yb. Therefore, it seems reasonable to specify the value of N as the degeneracy of the spin-orbit multiplet closest to the Fermi-energy. For Ce systems, one may estimate the value of Δ from photoemission data which shows that the width of the

incoherent peak at - 2 eV as being about 2 eV. Theory suggests that the width of the incoherent photoemission peak is given by $N \Delta$, since there are N channels for filling the empty 4f level and there are N channels each of which has a decay rate of Δ . For Ce, where the lowest spin orbit multiplet corresponds to $j=\frac{5}{2}$, the appropriate degeneracy is N=6, so $\Delta \sim \frac{1}{3}$ eV. The value of U for Ce is usually estimated from the joint photoemission/BIS spectrum as the energy difference between the incoherent peak (-2 eV) and the $4f^1 \rightarrow 4f^2$ peak (+4 eV) [see fig.(3)] which yields U=6 eV. Using the values of Δ inferred from experiment, one estimates that $U_c \sim 4 \text{ eV}$ for $n_f = 1$, but the critical value increases to 6.5 eV for a case of mixed-valence with $n_f \sim 0.8$. Comparison of the measured U with the critical value U_c leads to the conclusion that integer valent Ce systems should posses local magnetic moments but highly mixed-valent systems should not. Since the spin-orbit splitting between the $j=\frac{5}{2}$ and the $j=\frac{7}{2}$ levels is reversed in the last half of the lanthanide series, Yb $4f^{13}$ has a ground state configuration with $j=\frac{7}{2}$, so the 4f levels have a degeneracy of N=8. A typical value of Δ for Yb systems is estimated to be 0.15 eV. The value of U is approximately 6 eV as it is almost constant across the entire lanthanide series [17]. This implies that for Yb, the f occupancies which correspond to the non-magnetic state should be larger than $n_f \sim 13.72$.

The Hartree-Fock approximation is a reasonable approximation for small values of U and is exact in the atomic limit defined by V=0. It does provide a description of the high-energy spectral features but fails to describe a narrow low-energy peak close to the Fermi-energy associated with the Kondo effect.

However, the major problem with the above mean-field description is that it predicts phase transitions in which symmetry is broken. This is an artifact of the approximation; the properties of a finite system coupled to a Fermi-sea with an infinite number of degrees of freedom must change smoothly as the parameters are varied. Specifically, the fluctuations $\Delta n_{f,\alpha}$ are not negligible compared with the expectation values $\overline{n}_{f,\alpha}$ found in the mean-field approximation, due to the quantities being microscopic not macroscopic like the order-parameters that describe phase transitions in the thermodynamic limit. Hence, inclusion of fluctuations must restore the broken symmetry.

3.3 The Large Degeneracy Limit

The absence of magnetic states for mixed-valent systems with $n_T \leq 1$ is supported by a variational calculation which assumes that the Coulomb interaction U tends to infinity, so that the occupation number of the f level is restricted to be less than unity. The variational ansatz appropriate for the $U \to \infty$ limit was originally introduced by Varma and Yafet [18] for the case where N=2 but, following Anderson's remark [19] that the degeneracy N is responsible for stabilizing the non-magnetic state, has been generalized to the case of large N [20]. The ansatz for the non-

magnetic (singlet) state $|\Psi_0\rangle$ is expressed as

$$|\Psi_{0}\rangle = \left(A + \sum_{k,\alpha} B_{\underline{k}} f_{\alpha}^{\dagger} d_{\underline{k},\alpha}\right) |\Phi_{0}\rangle$$
 (28)

where $\mid \Phi_0 >$ represents the filled Fermi-sea of conduction electrons $k < k_F$, and A and $B_{\underline{k}}$ are variational parameters. The first term represents a state consisting of a filled Fermi-sea and an unoccupied f-level. The second term represents a linear superposition of states in which an electron has been taken from the filled Fermi-sea and placed in the f-level. It should be noted that both terms are non-magnetic, the second term is non-magnetic since it represents a state in which the electron with spin α is accompanied by a compensating polarization of the conduction electron spin density. On applying the variational method for the energy subject to the constraint that the state is normalized to unity, one finds two coupled equations

$$A (E - E_0) - \frac{1}{\sqrt{N_s}} \sum_{\underline{k},\alpha} V^*(\underline{k}) f(\underline{k}) B_{\underline{k}} = 0$$

$$B_{\underline{k}} (E - E_0 - E_f + \epsilon_d(\underline{k})) - \frac{1}{\sqrt{N_s}} V(\underline{k}) A = 0 \quad (29)$$

where E_0 is the energy of the filled Fermi-sea and $f(\underline{k})$ is the Fermi-Dirac distribution function for the conduction band states. On defining the Kondo binding-energy k_B T_K as

$$E = E_0 + E_f - \mu - k_B T_K , \qquad (30)$$

one finds that the holes in the conduction band have an amplitude given by

$$B_{\underline{k}} = \frac{1}{\sqrt{N_s}} \left(\frac{V(\underline{k})}{\epsilon_d(\underline{k}) - \mu - k_B T_K} \right) A. \tag{31}$$

The Kondo binding-energy is then determined from

$$\mu - E_f + k_B T_K = \frac{N}{N_s} \sum_{k} \frac{|V(\underline{k})|^2 f(\underline{k})}{k_B T_K + \mu - \epsilon_d(\underline{k})}$$
 (32)

where, unlike in the expression for $S(\omega)$ for the non-interacting model, the summation over \underline{k} is cut off by the Fermi-function and, therefore, gives rise to a logarithmic dependence on T_K . On assuming a constant density of d states $\rho_d(\mu)$ per host site, one finds that the binding-energy is given by the solution of

$$\mu - E_f + k_B T_K \approx N |V|^2 \rho_d(\mu) \ln \left| \frac{W + \mu + k_B T_K}{k_B T_K} \right|$$
 (33)

where W is a cut-off energy of the order of the band width. This leads to the approximate expression for the Kondo temperature

$$k_B T_K \approx W \exp \left[\frac{E_f - \mu}{N \rho_d(\mu) |V|^2} \right]$$
 (34)

which for $\mu - E_f \gg \frac{N \Delta}{\pi}$ shows that the non-magnetic state has an exponentially small binding-energy when referenced to the energy of the nominally magnetic state.

A compensating polarization cloud that surrounds the local f moment originates from conduction states within an energy interval k_B T_K below the Fermi-energy, although it extends up to the conduction band edge. Its energy distribution $P(\epsilon)$, per channel, is given by

$$P(\epsilon) \approx \left(\frac{\Delta}{N \Delta + \pi k_B T_K}\right) \frac{k_B T_K}{(k_B T_K + \mu - \epsilon)^2}.$$
 (35)

The spatial form of the polarization cloud is given by

$$P(\underline{r}) = \frac{1}{N_s a^3} \sum_{\underline{k}, \underline{k}', \alpha} B_{\underline{k}'}^* B_{\underline{k}} \exp \left[i \left(\underline{k} - \underline{k}' \right) \cdot \underline{r} \right]$$
 (36)

where \underline{k} and \underline{k}' are both below the Fermi-surface, and exhibits Friedel oscillations with wave vector near 2 k_F shown in fig.(4), where k_F is the Fermi-momentum. However, the characteristic length ξ at which the

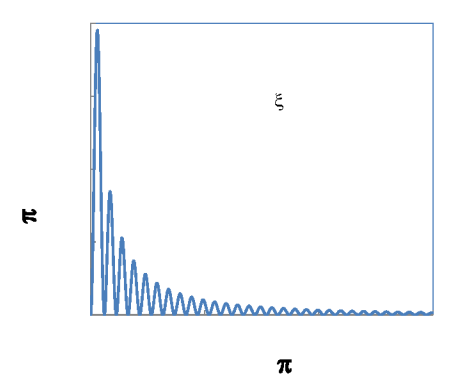


Figure 4: The schematic spatial variation of the polarization density, for N=4 and $k_F \xi \approx 10$.

interference due to Kondo correlations become apparent [21] is given by

$$k_F \xi = \frac{2 W}{k_B T_K} \,. \tag{37}$$

The length ξ is of the order of many hundreds of lattice spacings. In principle, the real-space structure of the Kondo screening cloud could be probed by nuclear magnetic resonance/Knight shift measurements on magnetic impurities dissolved into bulk metals. The total number of f electrons in the variational state is given by

$$n_{T} = \frac{N \sum_{k} |B_{\underline{k}}|^{2}}{|A|^{2} + N \sum_{k} |B_{\underline{k}}|^{2}}$$

$$\approx \frac{N \Delta}{N \Delta + \pi k_{B} T_{K}}$$
(38)

where we have assumed that $(W + \mu) \gg k_B T_K$. The total number of f electrons differs from unity by an exponentially small term which is proportional to the Kondo temperature. Equivalently, the relation between the Kondo temperature and the f occupation number can be expressed as

$$k_B T_K = \frac{\left(1 - n_T\right)}{n_T} \frac{N \Delta}{\pi} . \tag{39}$$

This suggests that, in the infinite U limit, the Kondo temperature can be viewed as being due to the renormalization of the rate Δ for a conduction electron from hopping onto the f level. The average value of the hopping rate is expected to be reduced by a factor of $(1 - n_T)$ since the Coulomb interaction will prohibit an electron to hop into a level that is already occupied.

The analysis of the nonmagnetic and magnetic states can be systematically extended to more complex variational functions in which the subsequent correction terms decrease in inverse powers of the degeneracy, if one scales Δ so that N Δ is considered as constant. While it is true that for cerium compounds $N^{-1} = \frac{1}{6}$ so the N^{-1} corrections can be considered as small, since the ratio $\frac{N\Delta}{U}$ is $\frac{1}{3}$, the finite U corrections appear to be more important [22].

3.4 The Schrieffer-Wolff Transformation

The single-impurity Anderson model is equivalent to the single-impurity s-d or Kondo model, in the limit where the set of f levels are only occupied by one electron. The equivalence was first shown by Schrieffer and Wolff [23] for the case N=2 and was generalized to finite N by Coqblin and Schrieffer [24]. The equivalence can be shown by writing the Hamiltonian for the single-impurity Anderson model as

$$\hat{H} = \hat{H}_0 + \hat{H}_{fd} \tag{40}$$

and then performing a canonical transformation

$$\hat{H}' = \exp\left[-\hat{A}\right] \hat{H} \exp\left[+\hat{A}\right] \tag{41}$$

where \hat{A} is an anti-Hermitean operator which is considered to be of the same order as \hat{H}_{fd} and still has to be determined. The transformed Hamiltonian \hat{H}' , when expanded in powers of \hat{A} , has the form

$$\hat{H}' = \hat{H}_0 + [\hat{H}_0, \hat{A}] + \hat{H}_{fd}
+ \frac{1}{2!} [[\hat{H}_0, \hat{A}], \hat{A}] + [\hat{H}_{fd}, \hat{A}] + \dots .$$
(42)

The operator \hat{A} is then chosen such that the terms in \hat{H}' which are first-order in the hybridization matrix element V vanish

$$[\hat{H}_0, \hat{A}] + \hat{H}_{fd} = 0.$$
 (43)

This leads to the transformed Hamiltonian being given by

$$\hat{H}' = \hat{H}_0 + \frac{1}{2!} [\hat{H}_{fd}, \hat{A}] + \dots$$
 (44)

which is accurate up to second-order in the hybridization matrix elements.

The anti-Hermitean operator \hat{A} can be written as

$$\hat{A} = \sum_{\underline{k},\alpha} \left[\hat{\Theta}_{\underline{k},\alpha} f_{\alpha}^{\dagger} d_{\alpha,\underline{k}} - \hat{\Theta}_{\underline{k},\alpha}^{\dagger} d_{\alpha,\underline{k}}^{\dagger} f_{\alpha} \right]$$
 (45)

where $\hat{\Theta}_{\underline{k},\alpha}$ is given by

$$\hat{\Theta}_{\underline{k},\alpha} = \sum_{n} P_{\alpha}^{n} \theta_{\underline{k},\alpha}^{n} \tag{46}$$

where P_{α}^{n} are operators which project on to the subspace where the set of (N-1) 4f states with quantum numbers $\beta \neq \alpha$ are occupied by n electrons. The complex numbers $\theta_{k,\alpha}^{n}$ are found as

$$\theta_{\alpha,\underline{k}}^{n} = -\frac{V^{*}(k)}{E_{f,\alpha} + Un - \epsilon_{d}(\underline{k})}. \tag{47}$$

Since the f levels are assumed to have a total occupancy of unity in the initial and final states, only the terms with n=0 and n=1 are needed. In the transformed basis, the interaction \hat{H}'_{int} between the f electrons and the conduction electrons as calculated to second-order in the hybridization can be reduced to

$$\hat{H}'_{int} = -\frac{1}{2 N_s} \sum_{\underline{k},\underline{k}',\alpha,\beta} \frac{V^*(\underline{k}) V(\underline{k}') U}{(E_f - \epsilon_d(\underline{k})) (E_f + U - \epsilon_d(\underline{k}))} f^{\dagger}_{\beta} f_{\alpha} d^{\dagger}_{\underline{k},\alpha} d_{\underline{k}',\beta}$$
(48)

which is the Coqblin-Schrieffer interaction. This interaction represents an exchange between the f electrons and the conduction electrons at the location of the impurity site. The interaction proceeds via virtual valence fluctuations involving both the non-occupied and doubly-occupied f states and has the strength

$$J_{k,k'} = \frac{V^*(\underline{k}) \ V(\underline{k'}) \ U}{(E_f - \epsilon_d(\underline{k})) \ (E_f + U - \epsilon_d(\underline{k}))}$$
(49)

which is negative. In the limit $U \to \infty$, the interaction strength reduces to

$$J_K \sim \frac{\mid V \mid^2}{\mid E_f \mid -\mu} \tag{50}$$

which also appears in the exponent of eqn. (34) that defined an approximate expression for the Kondo temperature. The Coqblin-Schrieffer interaction reduces to the Kondo interaction for the case N=2, apart from a potential scattering term at the impurity site.

The elimination of $(4f)^n$ configurations with $n \neq 1$ is reasonable when the 4f density of states is spilit into two peaks with characteristic energies far removed from the Fermi-energy. In this case, the virtual admixture of the higher-energy configurations into $(4f)^1$ can be neglected if the condition

$$\frac{\Delta}{\pi} \left[\frac{n_T}{\mu - E_f} + \frac{N - n_T}{E_f + U - \mu} \right] \ll 1 \tag{51}$$

is satisfied [7]. It should be noted that the Schrieffer-Wolff transformation does generate additional interactions that cannot be neglected in the mixed-valent limit. This is especially true for lattice models [25].

For N=2 the model can be mapped onto a spin one-half model by introducing the f spin-flip operators, \hat{S}^{\pm}

$$\hat{S}^{+} = f_{+}^{\dagger} f_{-}
\hat{S}^{-} = f_{-}^{\dagger} f_{+}$$
(52)

and defining the z-component of the spin \hat{S}^z via

$$\hat{S}^z = \frac{1}{2} \left(f_+^{\dagger} f_+ - f_-^{\dagger} f_- \right). \tag{53}$$

Likewise, one can introduce the spin density operators for the conduction electrons

$$\hat{\sigma}_{\underline{k},\underline{k}'}^{+} = d_{\underline{k},+}^{\dagger} d_{\underline{k}',-}
\hat{\sigma}_{\underline{k},\underline{k}'}^{-} = d_{\underline{k}',-}^{\dagger} d_{\underline{k},+}$$
(54)

etc. Using this notation and on enforcing the constraint

$$f_{+}^{\dagger} f_{+} + f_{-}^{\dagger} f_{-} = 1 ,$$
 (55)

one finds the interaction

$$\hat{H}'_{int} = -\frac{1}{N_s} \sum_{\underline{k},\underline{k}'} J_{k,k'} \underline{S} \cdot \underline{\sigma}_{\underline{k},\underline{k}'} - \frac{1}{4 N_s} \sum_{\underline{k},\underline{k}',\sigma} J_{k,k'} d^{\dagger}_{\underline{k}',\sigma} d_{\underline{k},\sigma} . (56)$$

The first term represents an interaction between the f spin and the spin of the conduction electrons at the impurity site. The second term represents potential scattering.

The finite U form of J_K has a simple explanation based on secondorder perturbation theory. If the localized f level is occupied by an electron with spin up, its energy is lowered by an amount

$$\Delta E_{\uparrow} \sim \frac{\mid V \mid^2}{E_f - \mu} \tag{57}$$

due to virtual hopping into the conduction band. However, the down-spin conduction electrons decrease their energy by an amount

$$\Delta E_{\downarrow} \sim \frac{\mid V \mid^2}{\mu - E_f - U} \tag{58}$$

due to virtual hopping into the f level leading it to be doubly-occupied which, therefore, involves the energy difference $E_f + U - \mu$. The sum of these energies is just J_K which represents an antiferromagnetic exchange interaction between the f electrons and the conduction electrons.

3.5 The Kondo Model

The s-d model [26] or Kondo model describes a localized spin with degeneracy (2S+1), which interacts with a single band of conduction electrons. The interaction can be written as

$$\hat{H}'_{int} = -\frac{1}{N_s} \sum_{\underline{k},\underline{k}'} J_K \underline{S} \cdot \underline{\sigma}_{\underline{k},\underline{k}'}. \tag{59}$$

The main difference between the Kondo and Coqblin-Schrieffer interactions is that in the Kondo model the localized spin can only change by amounts +1, 0 or -1, whereas in the Coqblin-Schrieffer Model the change is unrestricted. The s-d model was used by Kondo [27] to describe the resistivity minimum of metals containing magnetic impurities. His third-order perturbation approximation showed that the scattering rate for the conduction electrons diverged logarithmically at low temperatures. Furthermore, Abrikosov [28] showed that, on summing the leading logarithmic terms, the series diverges at T_K for negative J_K when

$$1 = 2 J_K \rho_d(\mu) \ln \left| \frac{k_B T_K}{W} \right|$$
 (60)

which defines the Kondo temperature for N=2. For positive J_K , the logarithmic terms suppress the interaction leading to the spin being free at zero temperature. A perturbative renormalization calculation by Anderson [29] also shows that at low T the antiferromagnetic model scales to strong coupling where the Kondo temperature is a scale invariant. Likewise for ferromagnetic coupling, the scaling trajectory leads to a ferromagnetic fixed point at which the spin-flip scattering vanishes. Extending Anderson's analysis to the Coqblin-Schrieffer model, one finds that the system scales to strong antiferromagnetic coupling $\rho_d(\mu) |J_{eff}| = \frac{1}{N}$ at the energy scale

$$k_B T_K = W e \left(N |J_K| \rho_d(\mu) \right)^{\frac{1}{N}} \exp \left[- \frac{1}{N |J_K| \rho_d(\mu)} \right]$$
 (61)

where e = 2.71828 is Napier's number.

When n_T is not too different from unity, models for mixed-valent impurities may be approximately described by Kondo models. In particular, like the Kondo model, all physical quantities may be expressed in terms of one single scale parameter, such as $\frac{N\Delta}{\mu-E_f}$. However, when n_T deviates significantly from unity, single parameter scaling may break down and physical properties may depend on N Δ and $\mu-E_f$ separately.

3.6 The Local Fermi-Liquid

Wilson's numerical renormalization group calculations for the Kondo model [30] show that, at sufficiently high temperatures, the interaction J_K can be treated as a perturbation. However, for negative J_K , as the temperature is lowered, the system undergoes a smooth cross-over to a state where J_K can be regarded as being infinitely strong. The strong coupling nature of the T=0 state had been previously inferred by Anderson [29] who used a perturbational renormalization technique. In this low temperature state, the antiferromagnetic nature of the Kondo coupling can be thought of as binding a compensating conduction electron cloud to the localized spin, resulting in a rigid singlet state [31]. Nozières [32] has pointed out that in this low temperature state, the other conduction electrons will experience a weak interaction mediated by virtual fluctuations of the singlet state. Furthermore, he pointed out that the non-bound conduction electrons can be described as a local Fermi-liquid.

At low temperature, the system settles into a Fermi-liquid state. The Fermi-liquid properties can be derived by considering the f electron self-energy $\Sigma_f(\epsilon)$. The inclusion of the Coulomb interactions results in the replacement

$$\epsilon - E_f + i \Delta \rightarrow \epsilon - E_f - \Sigma(\epsilon) + i\Delta$$
 (62)

in expressions involving the single-particle Green's function, such as the 4f density of states

$$\rho_f(\epsilon) = \sum_{\alpha} \rho_{f,\alpha}(\epsilon)$$

$$= -\frac{1}{\pi} \Im \left[\frac{N}{\epsilon - E_f - \Sigma(\epsilon) + i\Delta} \right]. \tag{63}$$

For low-energy excitations, one can expand in powers of $\epsilon - \mu$ leading to the approximation

$$\rho_f(\epsilon) \approx -\frac{1}{\pi} \Im \left[\frac{N}{Z(\epsilon - \mu) - E_f + \mu - \Sigma(\mu) + i\Delta} \right]$$
(64)

where Z is the wave function renormalization

$$Z = \left(1 - \frac{\partial \Sigma(\epsilon)}{\partial \epsilon} \bigg|_{\epsilon = \mu} \right) \tag{65}$$

and where we have used

$$\Im m \ \Sigma(\mu) = 0 \ . \tag{66}$$

The last equation follows since [33]

$$\Im m \ \Sigma(\epsilon) \ \propto \ (\epsilon - \mu)^2$$
 (67)

close to the Fermi-energy, which is a consequence of the limited phase space for producing particle-hole pairs. Hence, for ϵ in the vicinity of the Fermi-energy, the one-electron density of states can be expressed as

$$\rho_f(\epsilon) \approx -\frac{N}{\pi Z} \Im \left[\frac{1}{\epsilon - \tilde{E}_f + i\tilde{\Delta}} \right]$$
(68)

where

$$\tilde{E}_f = \frac{E_f + \Sigma(\mu) - \mu}{Z}$$

$$\tilde{\Delta} = \frac{\Delta}{Z} \tag{69}$$

are the renormalized f level energy and the renormalized hybridization lifetime. The Coulomb interactions result in the electronic excitations consisting of coherent quasiparticles which are in a one-to-one correspondence with the electrons of a non-interacting model, but which have a spectral weight of only Z^{-1} with Z > 1. The remaining spectral weight is transferred to higher energies such as the spectral features seen in fig.(3). However, following arguments originally due to Luttinger [33, 34], it has been proven [35, 36, 37] that the Friedel sum rule applies to the quasiparticle portion of the spectrum of the Anderson model. The total number of f electrons is given by

$$\frac{n_T}{N} = \frac{1}{\pi} \tan^{-1} \left(\frac{\tilde{\Delta}}{\tilde{E}_f - \mu} \right) \tag{70}$$

which reduces to the expression for the non-interacting model, as the wave function renormalization cancels out. This remarkable result leads to the f electronic density of states at the Fermi-level having the form

$$\rho_f(\mu) = \frac{N \sin^2(\frac{\pi n_T}{N})}{\pi \Lambda} \tag{71}$$

which is identical to the expression for the non-interacting model. Thus, the value of the density of states at the Fermi-energy is unchanged by the interactions. Furthermore, the fact that $\rho_f(\mu)$ is independent of U and the assumption that Z>1 guarantees that the density of states will have a peak in the vicinity of the Fermi-energy.

In the Kondo limit $n_T \to 1$, the wave function renormalization can be inferred from exact Bethe Ansatz calculations [38, 39, 40, 41], and is found to be

$$Z = \frac{\pi \Delta w_N}{k_B T_K} \left(\frac{N-1}{N^2 \sin^2 \frac{\pi}{N}} \right) \tag{72}$$

where w_N is the Wilson number [39] which is given by

$$w_n = \frac{\exp[1 + C - \frac{3}{2N}]}{2 \pi \Gamma(1 + \frac{1}{N})}$$
 (73)

where C is Euler's constant. For $\Delta \gg k_B T_K$, one sees that the wave function renormalization is much larger than unity. Once Z has been found,

the value of \tilde{E}_f can be found in terms of $\tilde{\Delta}$ from eqn.(70). This leads directly to the form of the low-energy portion of the electronic density of states. The low-energy density of states describes the Kondo peak or Abrikosov-Suhl resonance

$$\rho_f(\epsilon) = \frac{N}{Z \pi} \frac{\left(\frac{k_B T_K N^2 \sin^2 \frac{\pi}{N}}{\pi w_N (N-1)}\right)}{\left(\epsilon - \mu - \frac{k_B T_K N^2 \sin \frac{\pi}{N} \cos \frac{\pi}{N}}{\pi w_N (N-1)}\right)^2 + \left(\frac{k_B T_K N^2 \sin^2 \frac{\pi}{N}}{\pi w_N (N-1)}\right)^2}.$$
(74)

The Kondo peak (shown in fig.(5)) has an integrated intensity $\propto \frac{k_B T_K}{\pi w_N \Delta}$ and sits at an energy proportional to the Kondo temperature above the Fermi-surface. The width of the Kondo peak is also proportional to the Kondo temperature, but is significantly smaller than the excitation energy due to an N-dependent factor.

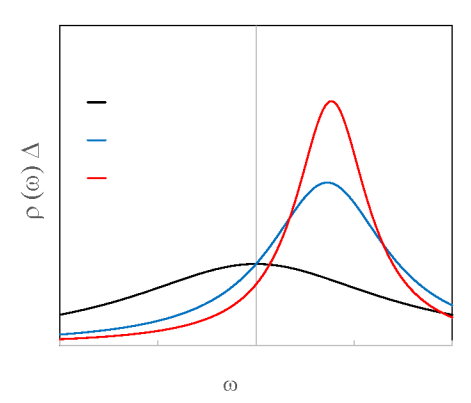


Figure 5: The energy dependence of the Abrikosov-Suhl resonance in the 4f density of states $\rho_f(\omega)$ where $\omega = \epsilon - \mu$, for various values of the degeneracy N.

In the Kondo limit, the wave function renormalization can be obtained by using Wilson's definitive relation between the Kondo temperature and the impurity's magnetic susceptibility [30] together with the relationship between the impurity's magnetic susceptibility and the coefficient of the linear T term in the impurity's electronic specific heat γ . The wave function renormalization can be then be found from γ , since γ is enhanced over the non-interacting value by a factor of Z when the self-energy is independent of \underline{k} . The various thermodynamic quantities that are required for this identification can be obtained from the Bethe Ansatz solution of the Coqblin-Schrieffer model.

For the integer valent limit or Coqblin-Schrieffer model, the zero temperature limit of the impurity's magnetic susceptibility [40] can be ex-

pressed as

$$\chi = (g\mu_B)^2 \frac{j(j+1) w_N}{3 k_B T_K} . (75)$$

The coefficient of the linear T term in the impurity's electronic specific heat term can be expressed as

$$\gamma = \pi^2 k_B^2 \frac{w_N}{3 k_B T_K} \frac{(N-1)}{N} . {(76)}$$

These two expressions, like all physical quantities in the Kondo limit, only depend on one single scaling parameter given by $\left(\frac{k_B}{w_N}\frac{T_K}{w_N}\right)$. On defining the Wilson ratio R for the impurity as

$$R = \frac{\pi^2 k_B^2}{j(j+1) (g\mu_B)^2} \left(\frac{\chi}{\gamma}\right),$$
 (77)

one finds that for the Coqblin-Schrieffer model [38, 40, 41], or equivalently for the Kondo limit of the degenerate Anderson model [42, 43, 44], R is calculated as

$$R = \frac{N}{(N-1)} \tag{78}$$

which differs from the value of unity expected from non-interacting electrons. The increased value of the ratio is due to a contribution to the susceptibility originating from the interactions between the quasiparticles in the different channels α . The numerical value R=2 was first obtained for the $S=\frac{1}{2}$ Kondo model by Wilson [30] from numerical renormalization group calculations. The ratio of 2 was subsequently re-derived analytically by Nozières [32] by applying concepts from Fermi-liquid theory. By combining the above relations, one obtains eqn.(72).

For mixed-valent systems the Wilson ratio differs from the simple ratio $\frac{N}{(N-1)}$ due to the presence of charge fluctuations. This can easily be proved by considering the magnetic susceptibility χ , the f charge susceptibility χ_c and the coefficient of the linear term in the specific heat γ . Starting from the expression for the magnetic susceptibility in the form

$$\chi = g \mu_B \sum_{\alpha} \alpha \left(\frac{\partial \overline{n}_{f,\alpha}}{\partial H} \right), \tag{79}$$

using the equation¹

$$\overline{n}_{f,\alpha} = \frac{1}{\pi} \tan^{-1} \left(\frac{\Delta}{E_f + \Sigma_{\alpha}(\mu) - \mu} \right)$$
 (80)

(like eqn.(70)) and on defining the chemical potential for electrons with quantum number α in a field via $\mu_{\alpha} = \mu + \alpha g \mu_{B} H$, one finds

$$\chi = (g\mu_B)^2 \sum_{\alpha,\alpha'} \alpha\alpha' \left(\delta^{\alpha,\alpha'} - \frac{\partial \Sigma_{\alpha}(\mu)}{\partial \mu_{\alpha'}} \right) \rho_{f,\alpha}(\mu) . \tag{81}$$

¹The equality of $\overline{n}_{f,\alpha}$ for all α is a consequence of the unbroken SU(N) symmetry, or equivalently, the singlet character of the ground state.

Due to the SU(N) symmetry, not only are all the self energies equal but all the off-diagonal $\alpha \neq \alpha'$ derivatives of the self energy $(\frac{\partial \Sigma_{\alpha}(\mu)}{\partial \mu_{\alpha'}})$ are also equal. Due to the symmetric distribution of the α around zero, only the diagonal terms $\alpha' = \alpha$ and the off-diagonal terms with $\alpha' = -\alpha$ remain after the summation over α' . Therefore, the susceptibility reduces to

$$\chi = (g\mu_B)^2 \sum_{\alpha} \alpha^2 \left(1 - \frac{\partial \Sigma_{\alpha}(\mu)}{\partial \mu_{\alpha}} + \frac{\partial \Sigma_{\alpha}(\mu)}{\partial \mu_{-\alpha}} \right) \rho_{f,\alpha}(\mu) . \tag{82}$$

Likewise, using the equality of all the (N-1) off-diagonal derivatives, one finds an expression for the charge susceptibility

$$\chi_{c} = \left(\frac{\partial n_{T}}{\partial \mu}\right)$$

$$= \sum_{\alpha} \left(1 - \frac{\partial \Sigma_{\alpha}(\mu)}{\partial \mu_{\alpha}} - (N - 1)\frac{\partial \Sigma_{\alpha}(\mu)}{\partial \mu_{-\alpha}}\right) \rho_{f,\alpha}(\mu) . \quad (83)$$

The off-diagonal derivatives cancel in the combination

$$(N-1) \frac{3 \chi}{(g\mu_B)^2 j(j+1)} + \chi_c = N \sum_{\alpha} \left(1 - \frac{\partial \Sigma_{\alpha}(\mu)}{\partial \mu_{\alpha}} \right) \rho_{f,\alpha}(\mu) . \tag{84}$$

We note that the coefficient of the linear T term in the specific heat is given by

$$\gamma = \frac{\pi^2 k_B^2}{3} \sum_{\alpha} \left(1 - \frac{\partial \Sigma_{\alpha}(\omega)}{\partial \omega} \Big|_{\omega=0} \right) \rho_{f,\alpha}(\mu)$$
 (85)

and that the self-energy rides on its own chemical potential ²,

$$\left(\frac{\partial \Sigma_{\alpha}}{\partial \omega}\right) = \left(\frac{\partial \Sigma_{\alpha}}{\partial \mu_{\alpha}}\right).$$
(86)

Therefore, one finds the equality

$$(N-1) \frac{3 \chi}{(g\mu_B)^2 j(j+1)} + \chi_c = N \frac{3 \gamma}{\pi^2 k_B^2}.$$
 (87)

In the Kondo limit, the charge fluctuations are suppressed so $\chi_c = 0$ and so one trivially recovers the Wilson ratio of $\frac{N}{(N-1)}$.

Bethe Ansatz calculations have been performed for the mixed-valent, degenerate, single-impurity Anderson model [42, 43, 44], in the limit $U \to \infty$. It was found that the magnetic susceptibility was composed of two contributions: one from the valence induced spin-fluctuations with energy

 $^{^2 \}text{The equality } \frac{\partial \Sigma_\alpha}{\partial \omega} = \frac{\partial \Sigma_\alpha}{\partial \mu_\alpha}$ follows from the observation that, since α is conserved, there is one chain of lines that runs throughout the self energy which can be labeled by α and by frequencies $\omega + \omega_s$. Since all other lines labeled by the quantum number α form closed loops, their contributions to $\frac{\partial \Sigma_\alpha}{\partial \mu_\alpha}$ cancel. Hence, since the propagators that contribute to the derivative with respect to μ_α only depend on the quantity $\omega + \mu_\alpha$, the equality follows.

scale Δ and the second from the Kondo fluctuations with an energy scale k_B T_K . In the mixed-valent regime, the results [45] are expressed in terms of the two energy scales Δ and the renormalized f-level energy E_f^* given by [46]

$$E_f^* = E_f + (N-1) \frac{\Delta}{\pi} \ln \frac{W}{\Lambda}$$
 (88)

Thus scaling requires two independent parameters. This can be seen from the leading exponential term in the expansion of the exact expression for the magnetic susceptibility [42]

$$\chi \approx \frac{\pi (g\mu_B)^2 j(j+1)}{3 N \Delta} \frac{\exp\left[+\frac{(E_f^* - \mu)}{N \Delta}\right]}{\Gamma(1 + \frac{1}{N})}$$
(89)

which depends on both N Δ and $\frac{(E_T^* - \mu)}{N}$ separately, as does the new scaling parameter T_H which describes the dependence on a magnetic field [43].

The crossover from the Kondo limit to the mixed-valent case is smooth, but sharpens for large N [42]. This can be seen by comparing the expression for the large N logarithm of the susceptibility with the large N expression for the number of f electrons n_T ,

$$n_T \approx 1 + \frac{1}{N} \left(\frac{N\Delta}{\pi(E_f^* - \mu)} \right) - \frac{1}{N} \left(\frac{N\Delta}{\pi(E_f^* - \mu)} \right)^2 \left(1 - \frac{1}{N} \right) \left[1 - \ln \left| \frac{N\Delta}{\pi(E_f^* - \mu)} \right| \right].$$
(90)

Combining the results, one obtains the expression [47]

$$\chi \sim \frac{\pi (g\mu_B)^2 j(j+1)}{3 N \Delta} \exp \left[\frac{1}{N (1-n_T)} \right]. \tag{91}$$

Thus, in the large N limit, χ appears to have an essential singularity as $n_T \to 1$, instead of the simple pole

$$\chi \sim \frac{\pi (g\mu_B)^2 j(j+1)}{3 N \Delta} \left(\frac{n_T}{1-n_T}\right)$$
 (92)

found with $\frac{1}{N}$ expansion methods (see fig.(6)).

One may also find an expression for the quasiparticle peak in the density of states for the mixed-valent case, for large N. This proceeds by noting that, if the charge susceptibility is to be positive, then the off-diagonal derivative $\frac{\partial \Sigma_{\alpha}(\mu)}{\partial \mu_{\alpha'}}$ must tend to zero when $N \to \infty$. In this case,

$$\chi = \frac{(g\mu_B)^2 j(j+1)}{3} Z \rho_f(\mu)$$
 (93)

which can be compared with the standard definition of the form of the mixed-valent magnetic susceptibility

$$\chi = \frac{(g\mu_B)^2 j(j+1) n_T}{3 k_B T_A}$$
 (94)

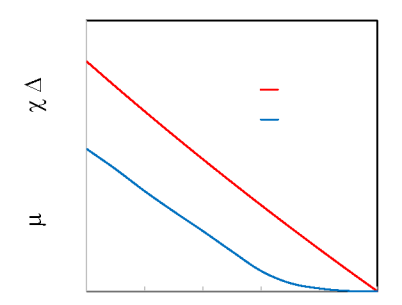


Figure 6: The dependence of χ^{-1} on n_T for N=8, (red line) leading N^{-1} expansion, (blue line) Bethe-Ansatz. (After Schlottmann [14])

where the factor n_T is included so that it is explicitly seen that $\chi \to 0$ when $n_T \to 0$. Hence, one may identify the wavefunction renormalization through

$$Z \rho_f(\mu) = \frac{n_T}{k_B T_A} . (95)$$

In the large N limit, the Friedel sum rule shows that Δ must scale as $\frac{1}{N}$ when compared to $\mu - E_f$. Thus,

$$\frac{n_T}{N} \sim \frac{1}{\pi} \frac{\tilde{\Delta}}{|\mu - \tilde{E}_f|} \tag{96}$$

while

$$\rho_f(\mu) = \frac{N}{\pi Z} \frac{\tilde{\Delta}}{|\mu - \tilde{E}_f|^2}$$

$$= \frac{1}{Z} \frac{n_T}{|\mu - \tilde{E}_f|}.$$
(97)

Therefore, $Z\rho_f(\mu)=\frac{n_T}{|\mu-\tilde{E}_f|}$. On using eqn.(95), one finds that the quasi-particle peak is centered at an energy

$$|\mu - \tilde{E}_f| = k_B T_A \tag{98}$$

with respect to the Fermi-energy. Then, the Friedel sum rule determines the width of the quasi-particle peak, $\tilde{\Delta}$, to be

$$\tilde{\Delta} = \pi \left(\frac{n_T}{N}\right) k_B T_A \tag{99}$$

Hence, close to the Fermi-energy, the large N one-electron density of states can be expressed as

$$\rho_{f}(\epsilon) = \frac{N}{\pi Z} \frac{\left(\frac{n_{T}\pi k_{B}T_{A}}{N}\right)}{(\epsilon - \mu - k_{B}T_{A})^{2} + \left(\frac{n_{T}\pi k_{B}T_{A}}{N}\right)^{2}}$$

$$= \frac{n_{T}k_{B}T_{A}}{\Delta} \frac{\left(\frac{n_{T}\pi k_{B}T_{A}}{N}\right)}{(\epsilon - \mu - k_{B}T_{A})^{2} + \left(\frac{n_{T}\pi k_{B}T_{A}}{N}\right)^{2}}$$
(100)

since the quasiparticle renormalization factor is given by

$$Z = \frac{N \Delta}{n_T \pi k_B T_A} . {101}$$

Thus, like in the Kondo limit, the T=0 one-electron density of states for a mixed-valent system consists of two prominent peaks far removed from the Fermi-energy and also has a small intensity quasiparticle peak of weight $\frac{1}{Z}$ with width $\propto \frac{k_B T_A}{N}$ that is located at an energy $k_B T_A$ measured from the Fermi-energy. In the Fermi-liquid regime, it can be shown that an increase in temperature results in a T^2 increase in Z and a shift in $|\mu - \tilde{E}_f|$ away from the Fermi-energy, all of which produces a "melting" of the quasiparticle peak.

4 Concentrated Compounds

Experimental results on concentrated mixed-valence and heavy-fermion compounds can frequently be described by the Anderson single-impurity model (See Section 6). However, generalization of the single-impurity theory to concentrated compounds runs into a number of major difficulties, such as saturation of the Kondo effect and the effect of interactions which may lead to magnetic ordering. These aspects are discussed below.

4.1 Nozieres Exhaustion

The spatial extent ξ of the screening cloud of conduction electrons surrounding a Kondo impurity is given by

$$k_F \xi = \frac{W}{k_B T_K} . ag{102}$$

The length scale is much greater than the lattice spacing. This is expected to put limitations on the application of the single-impurity models to concentrated compounds.

In particular, one expects that the Kondo impurities will start to interact when the compensating clouds start to interfere. This condition would suggest that interaction effects should first occur when the number of impurities N_{imp} satisfies

$$N_s a^3 \sim N_{imp} \xi^3 \tag{103}$$

where N_s is the number of lattice sites. Equivalently, this can be expressed as

$$N_{imp} \sim 6 \pi^2 N_{con} \left(\frac{k_B T_K}{W}\right)^3$$
 (104)

where N_{con} is the total number of conduction electrons. This condition suggests that interaction effects should set in for extremely small impurity concentrations. There is, however, no experimental evidence for such

interference effects in mixed-valent or heavy-fermion alloys or compounds.

A second limitation that has been suggested is the exhaustion principle [21]. The electrons that form the "compensating screening cloud" have energies of k_B T_K below the Fermi-energy. Hence, the maximum number of conduction electrons available to screen the impurity local moments, N_{eff} is estimated

$$N_{eff} = N_s \rho_d(\mu) k_B T_K \sim N_s \left(\frac{k_B T_K}{W}\right).$$
 (105)

Hence, this argument leads to the hypothesis that, when $N_{imp} > N_{eff}$, the number of conduction electrons is insufficient to screen the local moments. In particular, there would never be enough conduction electrons to screen a lattice of local magnetic moments, if one is to retain the picture of the single-impurity Kondo effect.

Nozieres has refined this picture by switching to a semi-classical time-domain argument and by making a key assumption [48], namely that the only relevant energy scale is set by the Kondo temperature, as in the single-ion Kondo effect. In particular, the number of conduction electrons N_{eff} that are available for screening local moments is assumed to be identical with the number found in the single-ion Kondo effect $(N_{eff} = N_s \ \rho(\mu) \ k_B \ T_K)$. These moment screening conduction electrons are itinerant and consecutively visit the magnetic sites producing precessions of the local moments that eventually result in an isotropic distribution of magnetic moments. The time scale τ at which a moment screening conduction electron, present at a magnetic site, produces a precession of the local moment by 2π about an axis is assumed to be given by

$$\tau = \frac{\hbar}{k_B T_K} \ . \tag{106}$$

The precession redistributes the moment's direction over a circular ring on the surface of the unit sphere. However, it requires visits by at least N electrons in order to redistribute the moment's direction over a solid angle of 4π .³ The coherence time τ_{coh} , defined as the time-scale for the randomization of the direction of every moment, is then given by

$$\tau_{coh} = (N-1) \left(\frac{N_{imp}}{N_{eff}}\right) \frac{\hbar}{k_B T_K}$$
 (107)

which leads to a coherence temperature T_{coh} given by

$$k_B T_{coh} = \frac{\hbar}{\tau_{coh}} \sim \frac{1}{(N-1)} \left(\frac{N_s}{N_{imp}} \right) \rho(\mu) (k_B T_K)^2.$$
 (108)

The distribution of moments is expected to have become isotropic and the system is expected to become non-magnetic below the coherence temperature. Nozieres's coherence scale can be much smaller than the single-ion

 $^{^{3}}$ The (N-1) different precessions or visits by (N-1) electrons, should be sufficient to destroy all the time-dependent phase relations between the components of the spinor.

Kondo temperature for large impurity concentrations.

The above argument leads to the conclusion that there exists more than one relevant energy scale for concentrated compounds, which in turn implies that they are governed by physics other than that contained in the single-impurity Kondo model. This undermines Nozieres's assumption that there is just one relevant energy scale [49]. Further guidance is given by mean-field calculations for the Kondo or Anderson Lattice Models of the type discussed in section (5.1), for which $N_s = N_{imp}$. These calculations indicate the existence of two related energy scales \tilde{V} and $|\tilde{V}|^2 \rho(\mu)$. The last scale represents both the single-impurity Kondo temperature which marks the temperature of the onset of moment loss

$$k_B T_K = |\tilde{V}|^2 \rho(\mu) \tag{109}$$

and the T=0 lowering of the ground state energy due to the coherent hybridization of the bands. Nozieres's argument can be modified by assuming that only electrons within \tilde{V} of the Fermi-energy participate in the screening of moments and that the energy scale for precession is also given by \tilde{V} . These substitutions result in a coherence scale that is given by

$$k_B T_{coh} = \frac{k_B T_K}{(N-1)}$$
 (110)

This coherence scale is a factor of N^{-1} times smaller than the Kondo scale, in agreement with a scale inferred from mean-field calculations for the Anderson Lattice Model [50]. This argument could imply that all that is needed to destroy coherent hybridization (i.e. produce $\tilde{V}(k) = 0$) at the Kondo temperature T_K is that the contributions to V from each site have randomized overall phases and does not require the randomization of each individual component of the spinors.

4.2 Doniach's Diagram

Heavy-fermions metals are frequently found in the vicinity of quantum critical points, and can be phenomenologically described by the Doniach's diagram [51]. Doniach's diagram is a statement about the relative energy scales of a lattice of magnetic ions which interact with the conduction electrons via a Coqblin-Schrieffer exchange interaction J_K . For an isolated impurity, the Kondo temperature is given by

$$k_B T_K \sim W \exp \left[-\frac{1}{N |J_K| \rho_d} \right],$$
 (111)

For temperatures below the Kondo temperature, an isolated local moment will be compensated by the magnetization of a screening cloud of conduction electrons leading to a singlet state. The Kondo effect competes with magnetic ordering promoted by an RKKY-like interaction which is second-order in the Kondo interaction. The RKKY-like interaction between two local moments has a magnitude of ρ_d J_K^2 [52]. A spontaneous magnetic fluctuation δm at one site, will generate an effective local field

of order ρ_d J_K^2 δm at a second site. The response at the second site has a magnitude of χ ρ_d J_K^2 δm , where χ is an appropriately reduced magnetic susceptibility, so $\chi \sim \frac{w_N}{k_B T_K}$. If the response at the second site is amplified, it can be expected that the system will become unstable. Otherwise, if the response at the second site is diminished, the system may be expected to be stable. Consideration of the ratio of the two energy scales suggests that, for the smallest values of ρ_d $|J_K|$, a magnetic phase will be stable. However, for N>1, a non-magnetic state will result at larger ρ_d $|J_K|$. A quantum critical point will separate the two phases. Since heavy-fermion systems are phenomenologically characterized by exceptionally small Kondo temperatures $1\gg \rho_d$ T_K , one infers that heavy-fermion materials are to be found near quantum critical points. On the other hand, mixed-valent materials should be found on the non-magnetic side, well-away from the critical point.

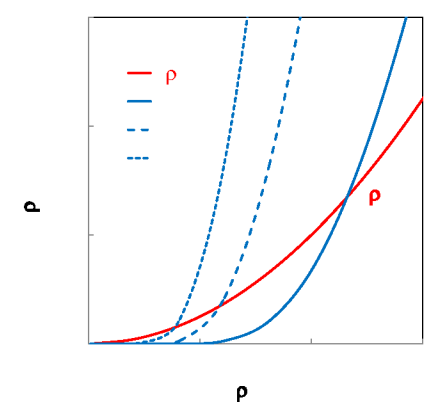


Figure 7: The Doniach phase diagram in which the dimensionless RKKY interaction $(\rho_d J_K)^2$ and the dimensionless Kondo temperature ρ_d $k_B T_K$ is plotted as a function of the magnitude of the Kondo exchange interaction $\rho_d |J_K|$, for various values of the degeneracy N. The value of N=3 is shown for clarity, but should be considered as unphysical.

Mean-field calculations on a lattice of Kondo impurities, interacting via antiferromagnetic intersite exchange interactions [53] lend support to the above arguments. The Kondo temperature T_K for the lattice is significantly different from that of an isolated impurity, and is strongly dependent on the concentration of conduction electrons. Furthermore, the Kondo phase terminates abruptly for low numbers of conduction electrons and strong intersite interactions.

5 The Anderson Lattice Model

Mixed-valent compounds which have an f ion in each unit cell can be modeled by the Anderson Lattice Model. In this model, there is a 4f ion at every lattice site which hybridizes with the conduction bands. The Hamiltonian can be expressed as

$$\hat{H} = \hat{H}_f + \hat{H}_d + \hat{H}_{fd} \tag{112}$$

where \hat{H}_f governs the lattice of f ions, \hat{H}_d describes the conduction band and \hat{H}_{fd} describes the hybridization process. The localized f orbital is described by a Hamiltonian \hat{H}_f

$$\hat{H}_f = \sum_{i,\alpha} E_{f,\alpha} f_{i,\alpha}^{\dagger} f_{\alpha} + \frac{U}{2} \sum_{i,\alpha \neq \beta} f_{i,\alpha}^{\dagger} f_{i,\alpha} f_{i,\beta}^{\dagger} f_{i,\beta}$$
(113)

where $f_{i,\alpha}^{\dagger}$ and $f_{i,\alpha}$, respectively, create and destroy an electron in the f-orbital on the lattice site labeled by i and α , $E_{f,\alpha}$ is the binding-energy and U is the screened Coulomb interaction between pairs of f electrons on the same lattice site. The Pauli-principle excludes an interaction between a pair of electrons in the same single-particle state $\alpha=\beta$ on the i-th f ion. As before, we shall consider the SU(N) model where the index α represents the combined spin and orbit quantum numbers which run over N values. The conduction electron Hamiltonian is denoted by \hat{H}_d and is given by

$$\hat{H}_d = \sum_{\underline{k},\alpha} \epsilon_d(\underline{k}) \ d^{\dagger}_{\underline{k},\alpha} \ d_{\underline{k},\alpha} \tag{114}$$

where $d_{\underline{k},\alpha}^{\dagger}$ and $d_{\underline{k},\alpha}$, respectively, create and destroy an electron in the Bloch state labeled by wavevector \underline{k} and quantum number α with the single-particle Bloch energy $\epsilon_d(\underline{k})$. The f states are coupled to the conduction states by the hybridization term \hat{H}_{fd} , given by

$$\hat{H}_{fd} = \sum_{\underline{k},\alpha} \left(V(\underline{k}) f_{\underline{k},\alpha}^{\dagger} d_{\underline{k},\alpha} + V^{*}(\underline{k}) d_{\underline{k},\alpha}^{\dagger} f_{\underline{k},\alpha} \right)$$
(115)

where $f_{\underline{k},\alpha}^{\dagger}$ and $f_{\underline{k},\alpha}$, respectively create and destroy electrons in the f state labeled by the Bloch wavevector \underline{k} and α . Unlike the impurity model, crystal momentum is conserved in the hybridization process. For the SU(N) model, α is conserved by the hybridization process.

The model can be solved in the limit where $U \to 0$. In this limit, the electronic structure consists of two sets of N-fold degenerate bands of mixed f and d characters with dispersion relations given by

$$E_{\alpha,\pm}(\underline{k}) = \frac{1}{2} \left(E_{f,\alpha} + \epsilon_d(\underline{k}) \pm \sqrt{(E_{f,\alpha} - \epsilon_d(\underline{k}))^2 + 4 |V(\underline{k})|^2} \right).$$
(116)

The f weight of the hybridized states is given by

$$|A_{\alpha,\pm}(\underline{k})|^2 = \frac{1}{2} \left(1 \mp \frac{(E_{f,\alpha} - \epsilon_d(\underline{k}))}{\sqrt{(E_{f,\alpha} - \epsilon_d(\underline{k}))^2 + 4 |V(\underline{k})|^2}} \right). (117)$$

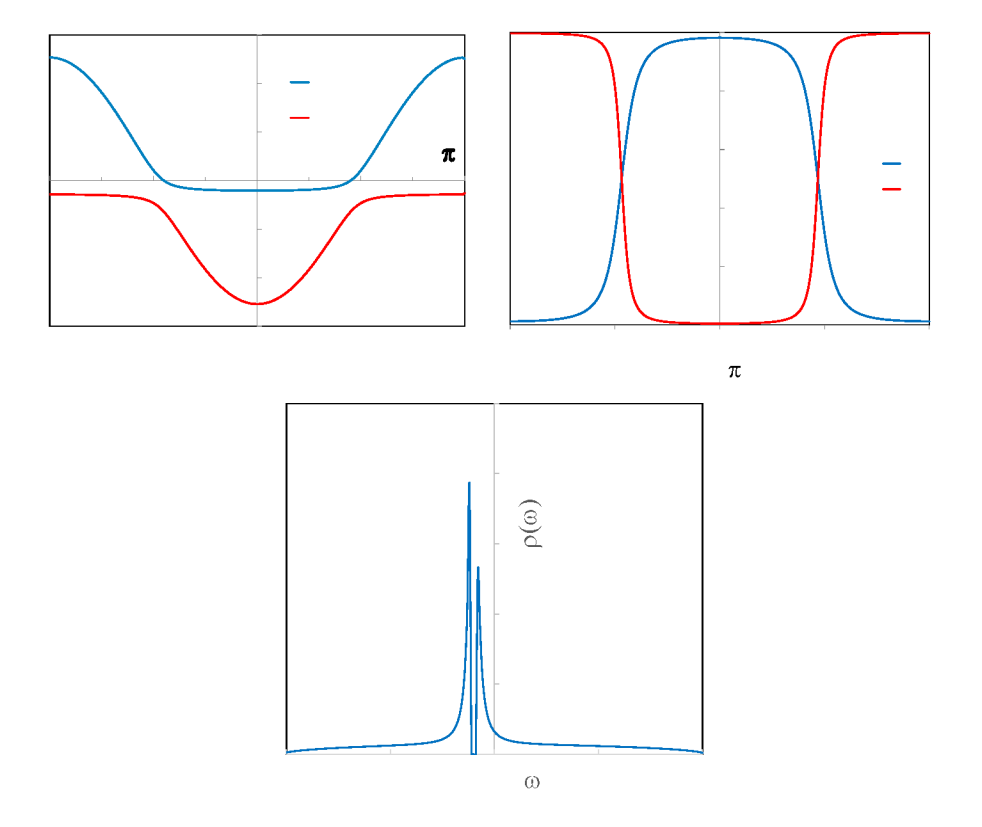


Figure 8: (a) A sketch of the electronic dispersion relations $E_{\pm}(\underline{k})$ for the non-interacting Anderson Lattice Model. (b) The f spectral weights $|A_{\pm}(\underline{k})|^2$ as a function of k. (c) The total density of states $\rho(\omega)$ divided by N versus ω .

The dispersion relation, the f spectral weight and density of states are sketched in fig.(8). From the dispersion relation, one sees that the two bands have a direct gap of 2 |V| but also have an indirect gap given by $4 |V|^2/W$, the hybridization gap. It is the coherent elastic scattering that is responsible for the gap in the spectrum. The f weight is distributed around E_f , but the indirect gap divides the f states into two parts. The Fermi-energy μ must necessarily be outside the indirect gap if the model is to describe a metallic system, even when the Coulomb interaction is present [34]. Otherwise, when the chemical potential is in the gap, the system is semiconducting and may describe Kondo Insulating materials [54].

The Anderson Lattice Model has been treated in the Dynamical Mean-Field Approximation (DMFA) [55, 56]. The DMFA maps the lattice model onto an effective single-impurity Anderson model where the effective conduction band density of states represents the effect of the environment

which includes the presence of the other f ions. The energy-dependence of the effective conduction band density of states has to be solved for self-consistency. The single-impurity problem then has to be solved either by Numerical Renormalization Group, Quantum Monte-Carlo [57] calculations or large N approximations [58]. The mapping onto a single-impurity model is motivated by the limit of infinite number of dimensions of the lattice $d \to \infty$, in which correlations between two lattice sites is washed out [55]. Therefore, the approximation should be reasonable whenever the electronic correlations are predominantly local.

5.1 The Slave-Boson Method

The $U \to \infty$ limit of the Anderson Lattice Model has been investigated by using the slave boson method [59]. The slave boson method was initially developed to treat the degenerate single-impurity Anderson model [60, 61] and, unlike other large N approaches to single-impurity model such as the Non-Crossing Approximation (NCA) [58], can be systematically applied to lattice problems.

The slave boson method is based on the observation that, as $U \to \infty$, it becomes energetically prohibitive to have multiply occupied f states on any ion and one must project out all the multiply occupied states whether they are physical or virtual. In the method [60, 61], the f electron operators $(f_{i,\alpha}^{\dagger}$ and $f_{i,\alpha})$ are replaced by the product of f quasiparticle operators $(\tilde{f}_{i,\alpha}^{\dagger}$ and $\tilde{f}_{i,\alpha})$ with the slave boson operators $(b_i^{\dagger}$ and $b_i)$, according to the prescription

$$f_{i,\alpha}^{\dagger} \rightarrow \tilde{f}_{i,\alpha}^{\dagger} b_{i}$$

 $f_{i,\alpha} \rightarrow b_{i}^{\dagger} \tilde{f}_{i,\alpha}$ (118)

The f quasi-particle operators are fermion operators which satisfy anticommutation relations, only if one enforces the constraint

$$\sum_{\alpha} \tilde{f}_{i,\alpha}^{\dagger} \ \tilde{f}_{i,\alpha} \ + b_i^{\dagger} \ b_i = 1 \tag{119}$$

at each site i. Since the eigenvalues of the boson number operators are limited to the set of positive integers supplemented by zero, this constraint eliminates multiply occupied f states at site i and results in

$$1 \geq n_T \geq 0 . \tag{120}$$

This constraint can be enforced by using Lagrange's method of undetermined multipliers λ_i . Lagrange's method produces an effective Hamiltonian similar to the original Anderson lattice Hamiltonian in which the Coulomb term has been projected out, but in which

$$E_f f_{i,\alpha}^{\dagger} f_{i,\alpha} \rightarrow (E_f + \lambda_i) \tilde{f}_{i,\alpha}^{\dagger} \tilde{f}_{i,\alpha}$$

$$V f_{i,\alpha}^{\dagger} d_{k,\alpha} \rightarrow V \tilde{f}_{i,\alpha}^{\dagger} d_{k,\alpha} b_i.$$
(121)

The effective Hamiltonian also contains the non-interacting boson Hamiltonian

$$\hat{H}_b = \sum_i \lambda_i \ b_i^{\dagger} b_i \tag{122}$$

The mean-field approximation, which is exact for the single-impurity model when $N \to \infty$, assumes that the boson field enters into a condensate at low temperatures. In this case, the condensate can be considered as an eigenstate of the operators b_i^{\dagger} and b_i and so the boson operators can be replaced by the complex numbers b^* and b.

On applying the mean-field slave boson method to the lattice [59] and only imposing the constraint on average, one finds that the hybridization matrix elements are renormalized according to

$$V \to \tilde{V} = V b \tag{123}$$

where b is a complex number, which satisfies the constraint

$$|b|^2 = (1 - n_T). ag{124}$$

In the above equation we have made use of Luttinger's theorem which ensures that the number of f electrons, n_T , is equal to the number of quasiparticles. The magnitude of b is found by minimizing the effective Hamiltonian with respect to b. The minimization results in the equation

$$\lambda b^* + \frac{1}{N_s} \sum_{\underline{k},\alpha} V(\underline{k}) < \tilde{f}_{\underline{k},\alpha}^{\dagger} d_{\underline{k},\alpha} > = 0$$
 (125)

which has to be solved self-consistently together with the constraint. For the lattice model, the chemical potential μ has also to be adjusted to keep the total number of electrons constant. The non-trivial solution, for which $b \neq 0$, yields a renormalization of the energy of the f level

$$E_f \to \tilde{E}_f = E_f + \lambda . \tag{126}$$

The renormalization of E_f and V have the effect of minimizing the Coulomb interaction. The inclusion of λ in \tilde{E}_f raises the f quasiparticle energy above the Fermi-energy and, therefore, reduces the interaction energy. The renormalization of V reduces the rate at which conduction electrons can hop into an f state $(\alpha \mid V \mid^2)$ by a factor of $\mid b \mid^2 = (1-n_T)$ which reflects the average effect of the Coulomb blocking hopping which would produce multiply occupied f orbitals. This renormalization is similar to the renormalization of Δ found for the $U \to \infty$ limit of the single-impurity model as expressed in eqn.(39).

5.2 The Coherent Fermi-Liquid

The self-consistent equations only have the trivial solution b=0 for temperatures above a characteristic temperature determined from

$$E_f - \mu \approx \frac{N \Delta}{2 \pi} \int_{-W}^{W} d\epsilon \left(\frac{2 f(\epsilon) - 1}{\epsilon - \mu} \right)$$
 (127)

since the chemical potential is pinned to the energy \tilde{E}_f of the partially occupied f quasiparticle level when $b \to 0$. This temperature is identified as the Kondo temperature T_K for the lattice below which the conduction electrons start to screen the localized magnetic moments

$$k_B T_K \sim W \exp\left[\frac{\pi \left(E_f - \mu\right)}{\Delta}\right]$$
 (128)

and $n_T(T)$ starts decreasing from unity. This expression has been derived by assuming a flat conduction band. Using more realistic forms of the conduction band density of states shows that T_K decreases and finally vanishes as the conduction electron density decreases [50]. For temperatures below T_K , the solution with finite b becomes stable and the system starts condensing into a Fermi-liquid state. In the mean-field approximation, the cross-over from the high-temperature state to a low-temperature Fermi-liquid state resembles a mean-field phase transition in which $|b|^2$ is the order parameter. Fluctuations of the order parameter are expected to smooth out the cross-over. This is expected [62] since, if the phase of the complex number b is known precisely (as in the mean-field state), then the condensate must be a coherent state which involves a linear superposition of states with different numbers of bosons. In this case, due to the large fluctuations in the boson number, the constraint cannot be satisfied at every lattice site and b is certainly not a static field. However, the phase or gauge fluctuations do not affect physical properties. Anyway, since the fluctuations are of higher-order in N^{-1} , the situation is similar to that of the single-impurity model where the cross-over from integer valent to mixed valence is smooth but becomes abrupt when calculated to leading order in N^{-1} .

Below T_K , b is a function of temperature and continues evolving but saturates at a temperature T_{coh} at which the Fermi-liquid is fully-formed [50]. The coherence temperature T_{coh} is related to T_K by a factor which depends on the density of conduction electrons. In this sense, the dependence of T_K and T_{coh} on the number of conduction electrons lends support to the arguments of Noziéres [21].

Once \tilde{V} , \tilde{E}_f and μ have been found, the effective Hamiltonian can be diagonalized in exactly the same way as the non-interacting model. However, the indirect gap between the quasiparticle dispersion relations is reduced to $2\frac{|V|^2}{W}(1-n_T(T))$ and the direct gap has a magnitude of $2|V|\sqrt{1-n_T(T)}$. The first renormalization shows up in the enhancement of the quasiparticle mass which is manifest in numerous experimental quantities [62], such as in the amplitude of the de Haas - van Alphen oscillations, the coefficient of the linear T term in the specific heat γ , the magnetic susceptibility χ , a reduction of the width of the low-temperature quasiparticle Drude peak in the optical conductivity and a quadratic enhancement of the coefficient A of the T^2 term in the electrical resistivity. The second renormalization shows up in terms of a mid-infrared peak in the optical conductivity due to a direct $(q \approx 0)$ inter-quasiparticle-band transition. However, at T=0, all the Fermi-liquid properties can be ex-

pressed in terms of the coherence temperature scale, T_{coh} .

Millis and Lee [62] addressed Noziéres's question [21] as to whether the Kondo screening occurs in the lattice and obtained the analogue of the magnetic screening function P(r) for the itinerant particles. Like in eqn.(35) for the single-impurity, the correlation can be expressed as

$$P(\underline{r}) = \frac{1}{N_s \ a^3} \sum_{\underline{k},\underline{k}' < k_F} B_{\underline{k}} B_{\underline{k}'} \exp \left[i \left(\underline{k} - \underline{k}' \right), \ \underline{r} \right]$$
 (129)

However, since the f quasiparticles are it inerant which elastic scatter coherently, the functions B_k are given by

$$B_{\underline{k}} = \frac{\tilde{V}(\underline{k})}{\sqrt{(\tilde{E}_f - \epsilon_d(\underline{k}))^2 + 4 |\tilde{V}(\underline{k})|^2}}$$
(130)

Unlike the corresponding function for the single-impurity model which is maximized at the Fermi-surface $k=k_F,\,B_{\underline{k}}$ is maximized at the direct gap where $\epsilon_d(\underline{k})=\tilde{E}_f$ and which defines the small Fermi-surface (which would be realized if $\tilde{V}\equiv 0$). Millis and Lee determined the correlation length for the lattice ξ to be given by

$$k_F \xi = \frac{W}{\tilde{V}} \tag{131}$$

which, although much shorter that the correlation length for the single-impurity model (since $k_F \xi \sim \frac{W}{k_B T_K} \sim (\frac{W}{\bar{V}})^2$), is still greater than the lattice spacing. They also determine the number of electrons screening each itinerant magnetic moment and found that it was given by $\frac{\bar{V}}{W}$. They argued that this shows the physics of the lattice is different from that of a single-impurity and that it is the itinerant character of the f electrons which results in the paramagnetism.

Doniach [52] has investigated whether the effects of interparticle interactions can produce magnetic instabilities. He found that magnetic interactions are produced by high-energy processes which are proportional to the fourth power of the hybridization matrix element V. Although calculated for the lattice, this magnetic interaction has a resemblance to the RKKY interaction between magnetic impurities for which $J_{RKKY} \sim$ $J_K^2 \rho_d(\mu)$ since the Schrieffer-Wolff transformation leads to $J_K \sim \frac{V^2}{(\mu - E_f)}$. On scaling V^2 with a factor of N, the RKKY-like interaction become of order N^{-2} . By treating these interactions in the Random Phase Approximation, Doniach reproduced essentially the same criterion for magnetic instability that he had found previously [51], $J_{RKKY} \sim k_B T_K$. Evans [63] has extended this analysis by including small interaction processes (of the order of Z^{-1}) that occur between the quasiparticles of the lowtemperature Fermi-liquid state. Unlike Doniach's mechanism, which produces instabilities at temperatures T_N where $T_N > T_K$, the low-energy processes may tip the balance and produce magnetic instabilities at temperatures below the coherence temperature T_{coh} .

6 Comparison with Experiment

The magnetic susceptibility $\chi(T)$, the 4f occupation number n_f (as measured by L3 x-ray absorption), and the Q-averaged dynamic susceptibility $\chi''(E)$ (as measured by neutron scattering) of the intermediate valence (IV) compound CePd₃ are shown in fig.(9). The ground state occupation number $n_f \sim 0.75$ (implying a Ce valence $z = 4 - n_f = 3.25$) and the characteristic energy of the spin fluctuations ($k_B T_K \sim E_{max} = 55$ meV) are typical of IV compounds. [67] The linear coefficient of specific heat $\gamma = 29$ mJ/mol-K² is also typical, indicating that these materials have moderately heavy Fermi liquid ground states.

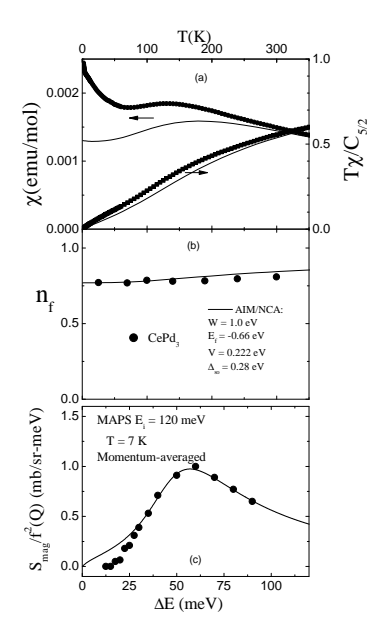


Figure 9: (a) The magnetic susceptibility; (b) the 4f occupation number as measured by L3 x-ray absorption; and (c) the low temperature polycrystalline-average neutron spectrum of CePd₃ compared to the predictions of the Anderson impurity model (solid lines) as calculated in the non-crossing approximation. The parameters for the bandwidth W, the f-level position E_f , the hybridization constant V, and the spin orbit splitting Δ_{so} are given in panel (b). (From Fanelli et al. [64])

These properties of Ce and Yb intermediate valence (IV) compounds can be fit simultaneously by the predictions of the Anderson impurity model (AIM). The solid lines in fig.(9) make this apparent for CePd₃. The low temperature specific heat coefficient (30 mJ/mol-K²) deduced from this calculation is basically equal to the experimental value. [64] The low temperature upturn in the susceptibility is an intrinsic coherence effect, as discussed further below. Similar fits are observed in YbAl₃ [66]

and YbAgCu₄ [65].

The Kondo temperature T_K in these compounds is large ($\sim 500 \text{ K}$) compared to typical rare earth crystal field energies, so that in the calculations the latter can be ignored and the Ce (Yb) atoms can be treated as $j=\frac{5}{2}$ $(j=\frac{7}{2})$ ions. Given the large T_K , these materials also are far from magnetic instabilities, so that the effects associated with a quantum critical point for a magnetic/nonmagnetic transition (viz., strong critical antiferromagnetic correlations) can be ignored. Under these circumstances, the physics is basically that of f electrons hybridizing with conduction electrons in the presence of strong Coulomb correlations - which in the impurity limit is the physics of the AIM. For the fits shown in fig. (9), the AIM was solved using the non-crossing approximation (NCA). [58] The results are moderately insensitive to the background bandwidth W. and the spin-orbit splitting Δ_{so} is fixed at the experimentally determined value so the fits depend essentially only on two parameters, the energy E_f of the 4f level and the hybridization parameter V. Given this latter fact, it is perhaps surprising that the impurity theory fits the data so well over such a large range of temperature and energy, particularly since the Ce (Yb) atoms are not impurities but sit on periodic cubic lattices in these compounds.

The measurements for which the AIM works well - $\chi(T)$, $n_f(T)$, $\gamma(T)$ and $\chi''(E)$ - are primarily sensitive to the local 4f fluctuations. For measurements that depend strongly on the lattice periodicity, this is not the case. While the high temperature resistivity of CePd₃ exhibits the negative $\frac{d\rho}{dT}$ expected for Kondo impurity behavior, at lower temperature the resistivity decreases with temperature, approaching (apart from extrinsic effects) $\rho=0$ at T=0 and exhibiting the T^2 behavior of a Fermi liquid (fig.(10)). This is the most obvious manifestation of the coherent behavior of the 4f lattice; similar low-T behavior is observed in all metallic IV compounds.

The appropriate model for localized f-electrons hybridizing with a single band of conduction electrons in the presence of strong Coulomb correlations is the Anderson lattice. As shown in section (5.2), in this model a hybridization gap sets in at low temperature and the bands have the same form as the non-interacting bands of fig.(8a) but with renormalized parameters \tilde{V} and \tilde{E}_f . The optical conductivity, which probes Q=0 excitations, then exhibits a peak in the mid infrared (the "mid-IR peak") on the scale of V. Okamura and collaborators [69] have shown that the mid-IR peak is endemic to Ce and Yb IV compounds, and the energy of the peak scales in an appropriate manner with the Kondo energy, as expected for the Anderson lattice. When the Fermi level lies in the region of high density of states (DOS) the system is a Fermi liquid with an enhanced effective mass. The optical conductivity then develops a Drude peak which is very narrow because the relaxation time is also renormalized. [70] As the temperature is raised, the f electrons decouple from the conduction electrons as the hybridization becomes increasingly less effective. At high temperature the conductivity no longer exhibits the mid-IR peak, but

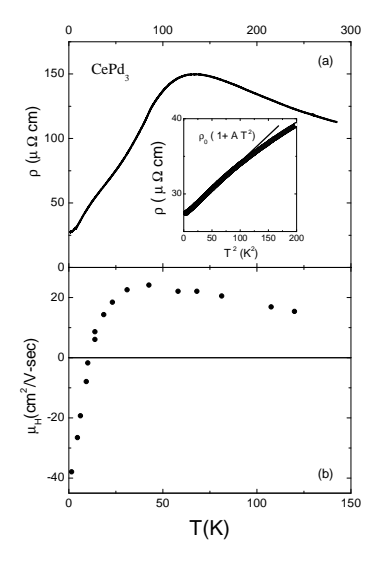


Figure 10: (a) The resistivity of CePd₃ as a function of temperature exhibits negative $\frac{d\rho}{dT}$ at high temperature, as expected for Kondo scattering, and T^2 behavior at low temperature (inset) as expected for a Fermi liquid. (From Fanelli [76]) (b) The Hall mobility of CePd₃ exhibits a dramatic change of behavior in the coherent Fermi liquid state below 50 K. (Adapted from Cattaneo *et al.* [68])

rather has a broad Drude response due to scattering of the conduction electrons from an incoherent set of f impurities. These two limits can be seen in the optical conductivity of CePd₃ (fig.(11)). Similar behavior is seen in other IV compounds such as YbAl₃. [71]

The optical conductivity of IV compounds gives a clear experimental example of the crossover from high temperature incoherent behavior to the coherent behavior of renormalized hybridized bands. Although the crossover occurs on a broad temperature scale (essentially that of the Kondo temperature), on a lower temperature scale T_{coh} the renormalization is essentially complete. As discussed in section (5.2), this is the temperature at which the order parameter saturates in slave boson theories. [50] Below the coherence temperature T_{coh} the growth of the mid-IR peak is complete, de Haas - van Alphen signals appropriate to the hybridized bands can be observed, and the resistivity shows the T^2 behavior expected of a Fermi liquid. The best-studied case is that of YbAl₃. Below 50 K, the mid-IR peak is completely established, the resistivity exhibits T^2 behavior, and the Hall coefficient exhibits a dramatic anomaly [66], similar to that seen in the Hall mobility of CePd₃ (fig.10), indicating an alteration of the Fermi surface. The de Haas - van Alphen signals at low temperature are those appropriate for a hybridized f band, with effective

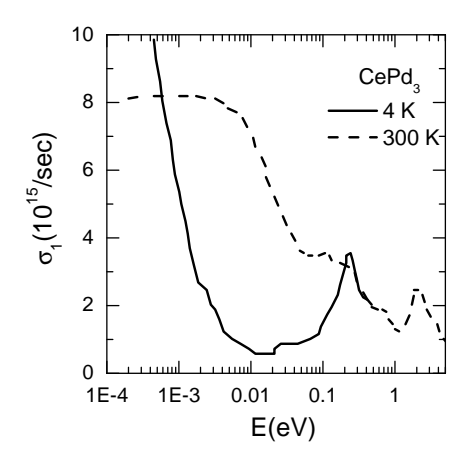


Figure 11: (a) The optical conductivity of CePd₃ at 300 and 4 K. (Adapted from Webb *et al.* [70]) The broad Drude behavior at high temperature transforms to the sum of a narrow Drude peak and a mid infrared peak on the scale \tilde{V} at low temperature.

masses in the range $m^* \sim 10 - 25m_e$. [72] The d.c. susceptibility also shows a small anomalous increase below this temperature. The similar increase seen in CePd₃ below 50 K (fig.(9a)) has been attributed [64] to the onset of a 5d contribution to the susceptibility reflecting coherent hybridization between the 4f and the 5d electrons in this compound.

Capturing the details of the hybridized ground state over the full Brillouin zone of actual IV materials requires going beyond the Anderson lattice model to correlated band theory, such as density functional theory where the correlations are treated in the dynamic mean field approximation [56] (DFT+DMFA). A recent calculation [73] for CePd₃ is shown in fig.(12). Clearly the most direct experiment to test this calculation would be angle-resolved photoemission on a single crystal. To our knowledge, however, such experiments have not been performed to date on the metallic rare earth IV compounds. On the other hand, the particle-hole excitations arising in the hybridized band structure can be measured by Q-resolved inelastic neutron scattering in single crystals. Since the intensity of the particle-hole excitation varies with the joint density of initial and final states, it will be strongest for excitations between flat regions of the bands of occupied and unoccupied states. In fig.(13), we show results for CePd₃ which show that on the Kondo scale (55 meV) the scattering is strongest for (1/2,1/2,0) momentum transfer and weakest

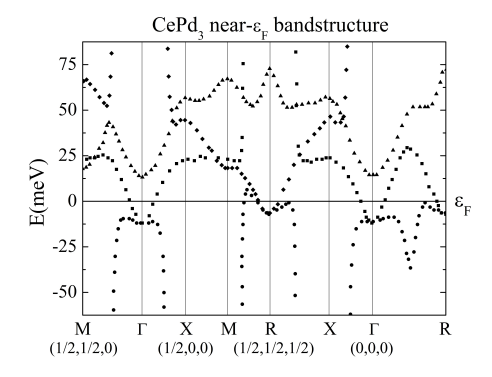


Figure 12: The correlated bandstructure of CePd₃ at low temperature as calculated using density functional theory and the dynamic mean field approximation. (Adapted from Sakai [73])

for (1/2,1/2,1/2). Below 40 meV the situation reverses: the scattering at (1/2,1/2,1/2) becomes larger than that at (1/2,1/2,0). (Similar variations of the Kondo scale scattering with Q have been observed in YbAl₃. [74]) While the energy scale of the excitations in the calculation appear to be somewhat smaller than that of the experiment, fig.(12) shows that the Γ /M transition with momentum transfer (1/2,1/2,0) should be strong at 40 meV, which is the Kondo scale in the calculation, while the Γ /R transition with momentum transfer (1/2,1/2,1/2) lies at an energy 90 meV which is larger than the energy window of fig.(13). The R/ Γ transition at 20 meV suggests that the (1/2,1/2,1/2) scattering should become larger than the (1/2,1/2,0) transitions below 40 meV, as we observe. Clearly a full calculation of the Q-dependent dynamic susceptibility is needed. However, this comparison between the neutron scattering and the correlated band theory is very encouraging in suggesting that the latter can quantitatively capture the behavior of real IV materials.

An important issue is why the Anderson impurity model works so well to describe much of the behavior of IV compounds. There are several reasons for this. The first, as mentioned above, is that the properties for which the AIM works well - the susceptibility, specific heat, Q-averaged neutron spectrum, and 4f occupation number - are primarily sensitive to local 4f fluctuations. The second is that the neutron scattering indicates that the variations with momentum transfer Q, while significant, are not enormous - the differences between the spectra seen in fig.(13) are only of order 20%. To the extent that these differences can be ignored, the spectra would be Q-independent, as for impurity scattering. This weak dependence on Q clearly is a product of the fact that the hybridized f bands are flat over appreciable regions of the Brillouin zone. Another important contribution to the quasi-Q-independence is the strong inelastic scattering expected in correlated systems. The states of the renormalized band theory are only sharp in energy or momentum at low temperatures and for energies close to the Fermi level. As the temperature and/or the

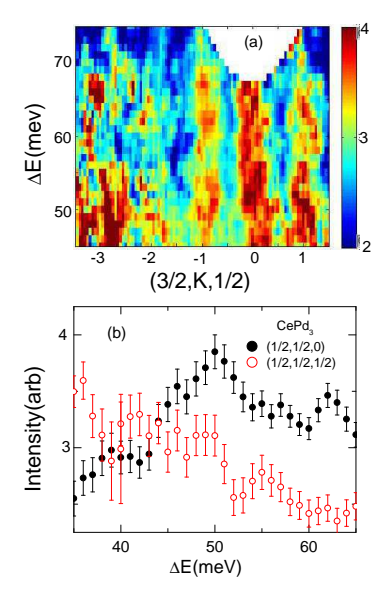


Figure 13: Inelastic neutron scattering spectra of a single crystal of CePd₃ as measured on the ARCS spectrometer at the Oak Ridge Spallation Neutron Source. The spectrum for momentum transfer (1/2,1/2,0) is more intense than that at (1/2,1/2,1/2) on the Kondo scale $(\Delta E \sim 55 \text{ meV})$ but weaker at energy transfer below 40 meV. (From Lawrence *et al.* [77])

distance of the energy from the Fermi level increases, the spectral functions rapidly become quite broad. The effect of this broadening has been shown to create a crossover to incoherent (Q-independent) behavior on a moderate temperature scale. [75] For example, we find that the neutron spectra of CePd₃ are already Q-independent at room temperature. [64] In any case, it is the weak Q-dependence which explains the applicability of the AIM to periodic IV compounds over a broad range of energy and temperature.

7 Summary

We have presented features of descriptions of intermediate or mixed-valent systems. Some of the descriptions that have been proposed were based on single-impurity models that, in the limit of almost integer f occupations, reduce to Kondo models. These impurity models have been extensively studied and many exact results have been derived, either through numerical renormalization group calculations, Bethe-Ansatz calculations or with Fermi-liquid theory. The degeneracy of the f orbital plays an important role in these descriptions. For large N, the smooth cross-over between mixed valence and the Kondo limit becomes rapid. We have also de-

scribed the features of a periodic array of mixed-valent atoms. Unlike the impurity models, exact results are scarce for lattice models. Nevertheless, like the impurity models, the degeneracy plays an important role in their description and, for large degeneracy, the cross-over between the high-temperature behavior (similar to that found in impurity models) to the low-temperature Fermi-liquid phase appears to be quite abrupt. Many of the experimental results on concentrated compounds can be described in terms of single-impurity models, despite theoretical arguments which question the applicability of single-impurity physics. Nevertheless, there are other features that are interpretable in terms of features of the lattice models.

Theories of lattice models of mixed-valent metals provide considerable opportunities for further developments. There is no exact theory and each of the various approximations that have provided so much insight into the mixed-valent lattice have their own limitations. Hartree-Fock [6], Random Phase Approximations [78] and the self-consistent and conserving [79] Fluctuation Exchange Approximation [80, 81, 82, 83, 84] (FEA) are only expected to be reasonable for sufficiently small values of the Coulomb interaction U. This condition is not met in the anomalous rare-earth compounds. Although valid at large U, mean-field slave boson theories run into difficulties in satisfying the constraints that exclude unphysical states. The Dynamical Mean-Field Approximation [55, 56] (DMFA) approximately maps lattice problems onto an effective single-impurity problem, which can then be iteratively solved with existing techniques. A result of the approximate mapping is that the spatial or momentum-dependence of the self-energy is washed out. This is perhaps not a great problem when discussing local properties, especially if the system is dominated by local correlations. However, it has been found [85] that non-local corrections due to the RKKY interaction can yield significant deviations from the electronic spectrum calculated in DMFA. DMFA methods [86, 87] take steps to address the deficiency of DMFA in treating spatial correlations, but so far have only been implemented with clusters containing a few nearest neighbor atoms. This hampers the application to situations such as in the vicinity of a quantum critical point, where long-ranged correlations are expected to develop. The combined use of the Local Density Approximation (LDA) to Density Functional Theory (DFT) with DMFA is a very positive and essential step towards the description of real materials. However, LDA+DMFA also raises new questions. Density Functional Theory is a theory which describes the ground state energy and the ground state density [88], if one has an appropriate non-local functional. The Kohn-Sham equation [89] used in DFT describes an effective single-particle problem, and the eigenvalues and eigenfunctions that are generated are artifacts which have no real physical meaning. The Kohn-Sham eigenfunctions only provide a method for generating an non-physical Slater determinant from which the ground state density can be obtained. If the Slater determinant were to be assigned a real physical meaning, then DFT would be reducible to a Hartree-Fock approximation and, therefore, would not be exact. Since the Coulomb correlations should have already been included in the Density Functional ground state, the inclusion of additional Coulomb interactions, such as U and J, in LDA+DMFA raises the question as to whether the effect of the correlations have been double-counted.

Many direct numerical investigations of finite-size correlated systems using exact diagonalization or quantum Monte Carlo methods have been performed. Exact diagonalization, has been severely limited by the exponential increase of computational effort required for increasing system size, while quantum Monte Carlo methods [90] have suffered from the fermionic minus sign problem at low temperatures. Due to these difficulties, and the vast number of states in Hilbert space needed to treat the degenerate Anderson Lattice, the work has hitherto been confined to consideration of one-band and low-dimensional models [91, 92]. Another difficulty faced by intensive numerical methods arises from their strong dependence on the finite-size of the lattices, which often has prevented the reliable extraction of the low-energy scales that are important for the description of strongly correlated systems. The great increase in computational power, combined with new efficient techniques show great promise for numerical approaches. The Density Matrix Renormalization Group (DMRG) is one such technique [93, 94], and is a generalization of Wilson's numerical renormalization group technique used to solve the single-impurity Kondo problem. This renormalization group technique is bases on iterative diagonalization of blocks of states and rescaling their interactions with neighboring blocks. In the DMRG technique, not all the low-energy states need to be kept on rescaling, but only those which make a substantial contribution to the density matrix. This results in a greater computational efficiency and optimizes the calculation of physical observables [95, 96, 97]. Another such approach is the continuous-time quantum Monte Carlo technique [98, 99, 100], which instead of sampling configurations in Hilbert space, samples terms in a diagramatic expansion of the partition function. However, the fermionic sign problem does remain [99]. The continuous time method offers the exciting possibility of studying the time-evolution of non-equilibrium correlated states. The rapid increase in computational power combined with technical improvements promises the production of accurate results for lattice models at low temperatures, which would be of prime interest for models which exhibit quantum critical behavior.

New results produced with newer methods combined with rigorous numerical results may provide a unifying picture of the physics of correlated hybridization problem which is at the core of mixed-valent physics. LDA+DMFT has made great progress in moving towards understanding real mixed-valence metals, and this progress should be continued by including interactions not already included in the simple Anderson Model picture. It is conceivable that close to a quantum critical point or far from equilibrium, these less conspicuous interactions could lead to the emergence of a rich variety of physical behavior that could be explored by future generations of researchers.

8 Acknowledgements

The work at Temple University was supported by the US Department of Energy, Office of Basic Energy Science, Materials Science through the award no. DE-FG02-01ER45872. Work by JML at Los Alamos was performed under the auspices of the U.S. Department of Energy, Office of Basic Energy Sciences, Division of Materials Sciences and Engineering. The work is dedicated to Ron Parks.

References

- [1] B. Coqblin, "The Electronic Structure of Rare Earth Metals and Alloys: The magnetic heavy rare-earths", Academic Press, London and New York (1977).
- [2] J.M. Lawrence, P.S. Riseborough and R.D. Parks, Rep. Prog. Phys. 44, 1-84 (1981).
- [3] M.A. Ruderman and C. Kittel, Phys. Rev. 96, 99-103 (1954).
- [4] T. Kasuya, Prog. Theor. Phys. 16, 45-57 (1956).
- [5] K. Yosida, Phys. Rev. **106**, 893-898 (1957).
- [6] P.W. Anderson, Phys. Rev. **124**, 41-53 (1961).
- [7] P. Noziéres and A. Blandin, J. de Physique, 41, 193-211 (1980).
- [8] B. Coqblin and A. Blandin, Adv. Phys. 17, 281-366 (1968).
- [9] N. Levinson, Kgl. Danske Videnskab Selskab. Mat. Fys. 25, 9, 1-29 (1949).
- [10] J. Friedel, Can. J. Phys. **34**, 1190-1211 (1956).
- [11] H.R. Krishnamurthy, J.W. Wilkins and K.G. Wilson, Phys. Rev. B,
 21, 1003-1043 (1980).
 H.R. Krishnamurthy, J.W. Wilkins and K.G. Wilson, Phys. Rev. B,
 21, 1044-1083 (1980).
- [12] N. Andrei, K. Furuya and J.H. Lowenstein, Rev. Mod. Phys. 55, 331-402 (1983).
- [13] A.M. Tsvelick and P.B. Wiegmann, Adv. Phys. 32, 453-713 (1983).
- [14] P. Schlottmann, Phys. Rep. 181, 1-119 (1989).
- [15] A.C. Hewson, "The Kondo Problem to Heavy Fermions", Cambridge University Press, Cambridge 1993.
- [16] A.C. Hewson and P.S. Riseborough, Solid State Commun. 22, 379-382 (1977).
- [17] J.K. Lang, Y. Baer and P.A. Cox, Phys. Rev. Lett. 42, 74-77 (1979).
- [18] C.M. Varma and Y. Yafet, Phys. Rev. B, 13, 2950-2957 (1976).
- [19] P.W. Anderson, "Valence Fluctuations in Solids", ed. L.M. Falicov, W. Hanke and M.P. Maple, (Amsterdam: North-Holland) p451, (1981).

- [20] O. Gunnarsson and K. Schönhammer, Phys. Rev. B, 28, 4315-4341 (1983).
- [21] P. Noziéres, Ann. de Phys. 10, 19-35 (1985).
- [22] O. Gunnarsson and K. Schönhammer, Phys. Rev. B, 31, 4815-4834 (1985).
- [23] J.R. Schrieffer and P.A. Wolff, Phys. Rev. 149, 491-492 (1966).
- [24] B. Coqblin and J.R. Schrieffer, Phys. Rev. 185, 847-853 (1969).
- [25] J.H. Jefferson, J. Phys. C: Solid State Phys. 10, 3589-3599 (1977).
- [26] C. Zenner, Phys. Rev. 81, 440-444, (1951).
- [27] J. Kondo, Prog. Theor. Phys. 32, 37-49 (1964).
- [28] A.A. Abrikosov, Physics, 2, 5 (1965).
- [29] P.W. Anderson, J. Phys. C, 3, 2436-2441 (1970).
- [30] K.G. Wilson, Rev. Mod. Phys. 47, 773-840 (1975).
- [31] K. Yosida, Phys. Rev. 147, 223-227 (1966).
- [32] P. Noziéres, J. Low. T. Phys. 17, 31-42 (1974).
- [33] J.M. Luttinger, Phys. Rev. 121, 942-949 (1961).
- [34] J.M. Luttinger, Phys. Rev. 119, 1153-1163 (1960).
- [35] D.C. Langreth, Phys. Rev. **150**, 516-518 (1966).
- [36] K. Yamada, Prog. Theor. Phys. 53, 970-986 (1975).
- [37] A. Yoshimori, Prog. Theor. Phys. 55, 67-80 (1976).
- [38] N. Andrei and J.H. Lowenstein, Phys. Rev. Lett. 46, 356-360 (1981).
- [39] A.C. Hewson and J.W. Rasul, Phys. Lett. **92A**, 95-98 (1982).
- [40] A.M. Tsvelick and P.B. Wiegmann, J. Phys. C: Solid State Phys. 15, 1707-1712 (1982).
- [41] A.C. Hewson and J.W. Rasul, J. Phys. C: Solid State Phys. 16, 6799-6815 (1983).
- [42] E. Ogievetski, A.M. Tsvelick and P.B. Wiegmann, J. Phys. C: Solid State Phys. 16, L797-L802 (1983).
- [43] P. Schlottmann, Z. Phys. B: Condensed Matter, 51, 223-235 (1983).
- [44] P. Schlottmann, Z. Phys. B: Condensed Matter, 54, 207-213 (1984).
- [45] P. Schlottmann, Z. Phys. B: Condensed Matter, 51, 49-59 (1983).
- [46] F.D.M. Haldane, Phys. Rev. Lett. 40, 416-419 (1978).
- [47] J.W. Rasul and A.C. Hewson, J. Phys. C: Solid State Phys. 17, 3337-3353 (1984).
- [48] P. Nozieres, Eur. Phys. J. B. 6, 447-457 (1998).
- [49] P. Nozieres, J. Phys. Soc. Japan, 74, 4-7 (2005).
- [50] S. Burdin, A. Georges and D.R. Grempel, Phys. Rev. Lett. 85, 1046-1051 (2000).
- [51] S. Doniach, Physica B, 91, 231-234 (1977).

- [52] S. Doniach, Phys. Rev. B, **35**, 1814-1821 (1987).
- [53] B. Coqblin, C. Lacroix, M.A. Gusmão and J.R. Iglesias, Phys. Rev. B, 67, 064417 (2003).
- [54] P.S. Riseborough, Adv. Phys. 49, 257-320 (2000).
- [55] W. Metzner and D. Vollhardt, Phys. Rev. Lett. 62, 324-327 (1989).
- [56] A. Georges, G. Kotliar, W. Krauth and M.J. Rozenberg, Rev. Mod. Phys. 68, 13-125 (1996).
- [57] A.N. Tahvildar-Zadeh and M. Jarrell, Phys. Rev. B. 55, R 3332-3335 (1997).
- [58] N.E. Bickers, D.L. Cox and J.W. Wilkins, Phys. Rev. B, 36, 2036-2079 (1987).
 N.E. Bickers, Rev. Mod. Phys. 59, 845-939 (1987).
- [59] P. Coleman, Phys. Rev. B, 35, 5072-5116 (1987).
- [60] S.E. Barnes, J. Phys. F: Metal Phys. 6, 1375-1383 (1976).
- [61] P. Coleman, Phys. Rev. B, 29, 3035-3044 (1984).
- [62] A.J. Millis and P.A. Lee, Phys. Rev. B, 35, 3394-3413 (1987).
- [63] S.M.M. Evans, J. Phys. Condensed Matter, 3, 8441-8456 (1991).
- [64] V.R. Fanelli, J.M. Lawrence, E.A. Goremychkin, R. Osborn, E.D. Bauer, K.J. McLellan, J.D. Thompson, C.H. Booth, A.D. Christianson and P.S. Riseborough, J. Phys. Condensed Matter, 26, 225602 (2014).
- [65] J.M. Lawrence, P.S. Riseborough, C.H. Booth, J.L. Sarrao, J.D. Thompson and R. Osborn, Phys. Rev. B, 63, 054427 (2001).
- [66] A.L. Cornelius, J.M. Lawrence, T. Ebihara, P.S. Riseborough, C.H. Booth, M.F. Hundley, P.G. Pagliuso, J.L. Sarrao, J.D. Thompson, M.H. Jung, A.H. Lacerda and G.H. Kwei, Phys. Rev. Lett. 88, 117201 (2002).
- [67] J. Lawrence, Modern Phys. Lett. B 22, 1273 (2008).
- [68] E. Cattaneo, U. Hafner and D. Wohlleben, in "Valence Instabilities", P. Wachter and H. Boppart, editors (North-Holland, 1982), page 451.
- [69] H. Okamura, T. Watanbe, M. Matsunami, T. Nishihara, N. Tsujii, T. Ebihara, H. Suguwara, H. Sato, Y. Onuki, Y. Isikawa, T. Takabatake and T. Nanba, J. Phys. Soc. Japan, 76, 023703 (2007).
- [70] B.C. Webb, A.J. Sievers and T. Mihalisin, Phys. Rev. Lett. 57, 1951-1954 (1986).
- [71] H. Okamura, T. Michizawa, T. Nanba and T. Ebihara, J. Phys. Soc. Japan, 73, 2045-2048 (2004).
- [72] T. Ebihara, Y. Inada, M. Murakawa, S. Uji, C. Terakura, T. Terashima, E. Yamamoto, Y. Haga, Y. Onuki and H. Harima, J. Phys. Soc. Japan 69, 895-899 (2000).
- [73] O. Sakai, J. Phys. Soc. Japan, 79, 114701 (2010).

- [74] A.D. Christianson, V.R. Fanelli, J.M. Lawrence, E.A. Goremychkin, E.D. Bauer, J.L. Sarrao, J.D. Thompson, C.D. Frost and J.L. Zarestky, Phys. Rev. Lett. 96, 117206 (2006).
- [75] X. Deng, J. Mravlje, R. Zitko, M. Fererro, G. Kotliar and A. Georges, Phys. Rev. Lett. 110, 086401 (2013).
- [76] V. Fanelli, Thesis, University of California, Irvine, 2009.
- [77] J.M. Lawrence, A.D. Christianson, R. Osborn, J.P. Castellan and M.B. Stone, unpublished data.
- [78] P.S. Riseborough and D.L. Mills, Phys. Rev. B, 21, 5338-5355 (1980).
- [79] G. Baym, Phys. Rev. **127**, 1391-1401 (1962).
- [80] N.E. Bickers and D.J. Scalapino, Ann. Phys. 193, 206-251 (1989).
- [81] N. Bickers, D. Scalapino and S. White, Phys. Rev. Lett. 62, 961-964 (1989).
- [82] N.E. Bickers and S.R. White, Phys. Rev. B, 43, 8044-8064 (1991).
- [83] P. G. McQueen, D.W. Hess and J.W. Serene, Phys. Rev. Lett. 71, 129-132 (1993).
- [84] P.G. McQueen, D.W. Hess and J.W. Serene, Phys. Rev. B, 50, 7304-7310 (1994).
- [85] Y. Shimizu, J. Phys. Soc. Japan, 71, 1166-1173 (2002).
- [86] M.H. Hettler, M. Mukherjee, M. Jarrell and H.R. Krishnamurthy, Phys. Rev. B, 61, 12739 (2000).
- [87] G. Kotliar, S. Savrasov, G. Palsson and G. Biroli, Phys. Rev. Lett. 87, 186401 (2001).
- [88] P. Hohenberg and W. Kohn, Phys. Rev. B, 136, 864-871 (1964).
- [89] W. Kohn and L.J. Sham, Phys. Rev. B, 140, 1133-1138 (1965).
- [90] J.M. Hirsch and R.M. Fye, Phys. Rev. Lett. 56, 2521-2524 (1986).
- [91] H. Tsunetsugu, Y. Hatsugai, K. Ueda and M. Sigrist, Phys. Rev. B 46, 3175 (1992)
- [92] R.M. Fye and D.J. Scalapino, Phys. Rev. Lett. 65, 3177-3181 (1990).
- [93] S.R. White, Phys. Rev. Lett. 69, 2863-2866 (1992).
- [94] U. Schollwock, Rev. Mod. Phys. 77, 259-315 (2005).
- [95] C.C. Yu and S.R. White, Phys. Rev. Lett. **71**, 3866-3869 (1993).
- [96] N. Shibata and K. Ueda, J. Phys. Condensed Matter, 11, R1-R30 (1999).
- [97] I.P. McCulloch, A. Juozapavicius, A. Rosengren and M. Gulacsi, Phys. Rev. B, 65, 052410 (2002).
- [98] N.V. Prokof'ev, and B.V. Svistunov, Phys. Rev. Lett. 81, 2514-2517 (1998).
- [99] S. Rombouts, K. Heyde and N. Jachowicz, Phys. Lett. A, 242, 271-276 (1998).
- [100] E. Gull, A.J. Millis, A.I. Lichtenstein, A.N. Rubtsov, M. Troyer and P. Werner, Rev. Mod. Phys. 83, 349-404 (2011).